# MOLECULAR DOCKING STUDY FOR NOVEL PHOSPHODIESTERASE-IV INHIBITORS

by

Gülşah Çifci

B.S., Chemistry, Boğaziçi University, 2008

Submitted to the Institute for Graduate Studies in
Science and Engineering in partial fulfillment of
the requirements for the degree of
Master of Science

Graduate Program in Chemistry
Boğaziçi University
2010

# ACKNOWLEDGEMENTS

I would like to express my sincere gratitude to my thesis advisor Prof. Dr. Viktorya Aviyente for her guidance, help, advice and patience. I would like to thank her for her continuous support to complete this work.

I wish to extend my appreciation to the members of my committee: Prof. İlknur Doğan and Assoc. Prof. Demet Akten for their valuable advices and comments.

My hearty thanks go to all the members of computational chemistry group, especially to my dear friend Tuğba Furuncuoğlu for her never-failing support, to Nihan Çelebi Ölçüm for her valuable advices, to İsa Değirmenci, İlke Uğur, Burcu Çakır Dedeoğlu, Sesil Agopcan, Şeref Gül, Özlem Karahan, Hasan İnce and Alican Gülsevin for being very helpful. I would like to thank the members of the faculty in Bogazici University Chemistry Department, especially Hülya Metiner for her invaluable helps.

I gratefully acknowledge Prof.Gerhard Wolber and Ph.D Simona Distinto (Innsbruck University, Austria) for their advices, comments and their scientific guidance during my stay in Computer-Aided Molecular Design Group (Innsbruck University, Austria) .

Finally, I would like to express deepest gratitude and respect to my family for their continuos support, understanding and love throughout my life.

# ABSTRACT


## MOLECULAR DOCKING STUDY FOR NOVEL PHOSPHODIESTERASE4 INHIBITORS

In this study, a molecular docking process for different Phosphodiesterase4 inhibitors is carried out.

In the molecular modeling field, the process of docking a ligand to a binding site consists in mimicing the natural course of interaction of the ligand and its receptor via a lowest energy pathway. Before the molecular docking, X-ray crystal structures for Phosphodiesterase-IV enzyme from the Protein Databank are analysed. According to crystal structures, four pharmacophores are designed with the LigandScout software and one of them is improved with the Catalyst program. Virtual screening based on this pharmacophore model is carried out with 6 databases which contain about 2 million drug-like compounds. At the end of virtual screening, 1959 hit compounds are found. According to physicochemical filters and Lipinski rule of five, some of the compounds are marked as non-druglike compounds and they are eliminated. The docking process is performed with AutoDock 4.0 for the remaining candidate compounds. During the docking process, the binding energies, the root mean square deviation (RMSD) values and $K_i$ (dissociation constant) are obtained for each compound. Based on these findings, some of the compounds are filtered. Finally the strain energy between the best pose of the ligands selected by AutoDock 4.0 and their optimized conformation are calculated with PM3 in Spartan.

# ÖZET


## YENİ PHOSPHODIESTERASE4 İNHİBİTÖRLERİ İÇİN MOLEKÜLER DOKLAMA İŞLEMİ

Bu çalışmada, farklı Phosphodiesterase4 inhibitörleri için moleküler doklama işlemi gerçekleştirildi.

Moleküler modelleme alanında, bir ligandı bağlanma bölgesine doklama süreci ligandın ve onun alıcısıyla en düşük enerji yoluyla etkileşimini, doğal akışını taklit etmeyi dener. Moleküler doklamadan önce, başlangıçta, Protein veritabanındaki Phosphodiesterase4 enzimi için X-ışını kristal yapıları analiz edildi. Kristal yapılarına göre, dört tane farmakofor, "LigandScout" yazılımıyla modellendi ve onların biri "Catalyst" programıyla geliştirildi. Bu farmakofor modeline gore sanal eleme 2 milyon ilaç benzeri bileşik içeren 6 tane veritabanıyla tamamlandı. Sanal elemenin sonunda, 1959 tane uygun bileşik bulundu. Fizikokimyasal filtrelere ve Lipinski kuralına göre, bileşiklerin bir kısmı, ilaç gibi olmayan bileşikler olarak işaretlendi ve onlar elendi. Doklama işlemi, elde kalan aday bileşikler için AutoDock 4.0'la yapıldı. Doklama süreci esnasında, her bileşik için bağlanma enerjileri, ortalama karesel sapma (RMSD) değerleri ve $K_i$ (ayrışma sabiti) elde edildi. Bu verilere göre, bileşiklerin bir kısmı elendi. Çalışmanın sonunda, AutoDock 4.0 tarafından üretilen ligandların en iyi pozuyla onların en iyi şekilde kullanılan biçimi arasındaki bükülme(zorlama) enerjisi PM3 metoduyla Spartan'da hesaplandı.

# TABLE OF CONTENTS

# LIST OF FIGURES

# LIST OF TABLES

# LIST OF SYMBOLS/ABBREVIATIONS

| | |
|---|---|
| *Ki* | Dissociation constant |
| $\Delta E$ | Strain energy |
| *PM3* | Parametrized Model Number 3 |
| *MMFF94x* | An all-atom forcefield parametrized for small organic molecules |

# 1. INTRODUCTION

## 1.1. Phosphodiesterase Enzyme

In 1962, Butcher and Sutherland identified phosphodiesterases as the enzymes responsible for the breakdown of adenosine 3',5'-monophosphate (cAMP) [1]. The discovery of the physiological importance of intracellular cAMP in mediating the effects of various hormones and the development of the concept of the 'second messenger' were rewarded in 1971 with a Nobel Prize to Sutherland and his coworkers.

Cyclic nucleotide phosphodiesterase (PDE) hydrolyzes adenosine or guanosine 3', 5'-cyclic monophosphate (cAMP or cGMP) to 5'-AMP or 5'-GMP [2-4]. Cyclic AMP and cyclic GMP are intracellular second messengers mediating the response of cells to a wide variety of hormones and neurotransmitters in signal transduction pathways.

Regulation of cAMP and cGMP concentration in vivo is an important step for many metabolic processes, like cardiac and smooth muscle contraction, glycogenolysis, platelet aggregation, secretion, lipolysis, learning, ion channel conductance, apoptosis, and growth control [5-7].

Up to now, 11 families and 21 genes of PDE's have been reported which were characterized by different substrate specificity (cAMP or cGMP), inhibition, substrate requirements, gene sequence, and tissue distribution [2, 5-6, 9-13].

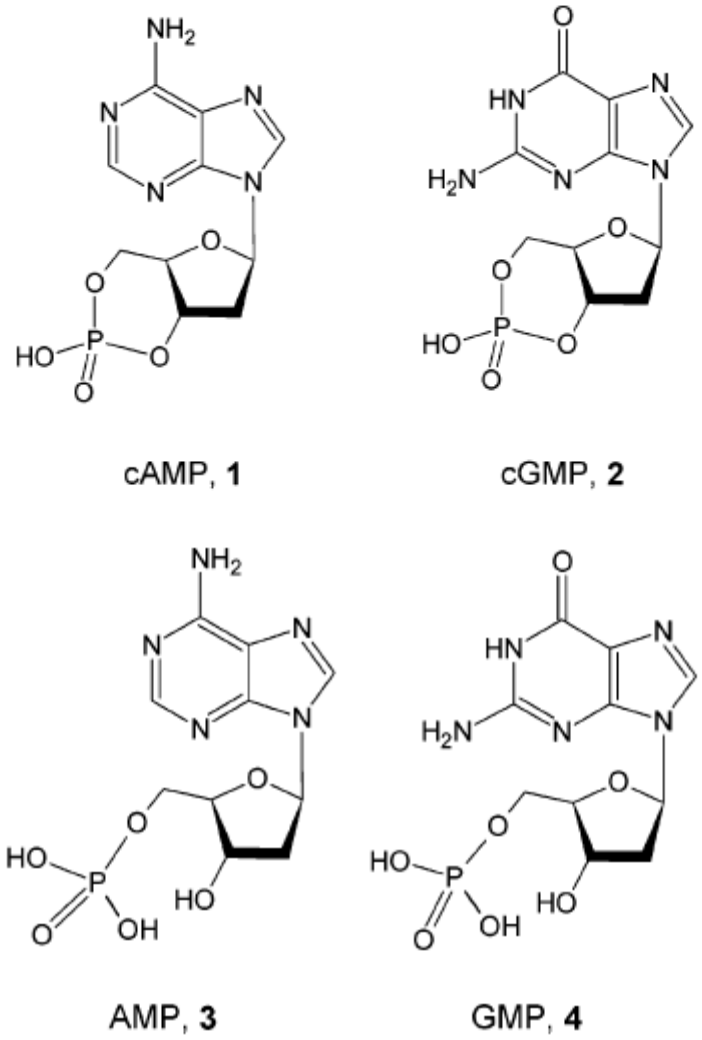


Figure 1.1 Cyclic Nucleotides, cAMP, cGMP, and products from PDE hydrolysis: AMP and GMP [8]

Table 1.1. Tissue distribution over 11 families of PDE enzymes

| |
|---|
| PDE1 ➔ Testes,brain,heart,vascular SMC |
| PDE2 ➔ CNS,adrenal cortex |
| PDE3 ➔ Adipose,cardiac muscle,liver |
| PDE4 ➔ Neural,endocrine,lung,mast cells |
| PDE5 ➔ Lung,platelets,kidney |
| PDE6 ➔ Retina(rod and cone cells) |
| PDE7 ➔ Skeletal muscle,T-lymphocytes |
| PDE8 ➔ Testes,ovary,intestine |
| PDE9 ➔ Spleen,kidney,heart,brain |
| PDE10 ➔ Brain,testes |
| PDE11 ➔ Prostate,skeletal muscle |

The mRNAs of the PDE genes are subject to alternative splicing, resulting in over 60 PDE isoforms in various human tissues. The families of PDE contain a conserved catalytic domain which has about 300 amino acids with an approximate 25% sequence homology. However, each PDE family recognizes a specific substrate and has its own selective inhibitors. Therefore, the families of PDE4, 7, and 8 are specific to cAMP, on the other hand PDE5, 6, and 9 prefer cGMP. PDE1, 2, 3, 10, and 11 take both cAMP and cGMP as their substrates [8].

Table 1.2. Cyclic nucleotide selectivity profile of the 11 PDE family members [14]

| PDE family | pharmacological classification | cyclic nucleotide substrates | inhibitors | $K_i$ or ($IC_{50}$) |
|---|---|---|---|---|
| PDE1 | $Ca^{2+}$/CAM stimulated PDE | cAMPand cGMP | vinpocetine | 14 μM |
| | | | zaprinast | (6 μM)[37] |
| | | | sildenafil | (350 nM)[38] |
| PDE2 | cGMP-stimulated PDE | cAMP and cGMP | EHNA | 1 μM |
| | | | Bay 60-7550 | (4.7 nM)[56] |
| PDE3 | cGMP-inhibited PDE | cAMP > cGMP | cilo8tamide | 20 nM |
| | | | milrinone | 150 nM |
| | | | zardaverine | (0.5-2 μM) |
| PDE4 | high affinity, rolipram-sensitive cAMP-specific PDE | cAMP | rolipram | 1 μM |
| | | | roflumilast | (0.8 nM)[45] |
| | | | cilomilast | (120 nM)[45] |
| | | | zardaverine | (0.8-4 μM) |
| PDE5 | cGMP-specific PDE | cGMP | zaprinast | 130 nM |
| | | | sildenafil | 10 nM |
| | | | vardenafil | 1 nM |
| | | | tadalafil | 10 nM |
| PDE6 | photoreceptor cGMP-specific PDE | cGMP | zaprinast | 400 nM |
| | | | dipyridamole | 125 nM |
| | | | sildenafil | 50 nM |
| | | | vardenafil | (11 nM)[38] |
| | | | tadalafil | (2 μM) |
| PDE7 | high-affinity, rolipram-insensitive cAMP-specific PDE | cAMP | IBMX | 4 μM |
| | | | dipyridamole | 600 nM |
| PDE8 | high-affinity, IBMX-insensitive cAMP-specific PDE | cAMP | dipyridamole | 9 μM |
| PDE9 | high-affinity cGMP-specific PDE | cGMP | zaprinast | 35 μM |
| PDE10 | cAMP-inhibited cGMP PDE | cAMP < cGMP | dipyridamole | 1 μM |
| | | | zaprinast | (22 μM)[36] |
| PDE11 | dual specificity cGMP-binding PDE | cAMP and cGMP | zaprinast | 12 μM |
| | | | dipyridamole | 0.4 μM |
| | | | tadalafil | 60 μM |

The selective inhibitors for different PDE families have been generally used as cardiotonic agents, vasodilators, smooth muscle relaxants, antidepressants, antithrombotic compounds, antiasthma compounds, and agents for improving cognitive functions such as memory in the past three decades [15-19].

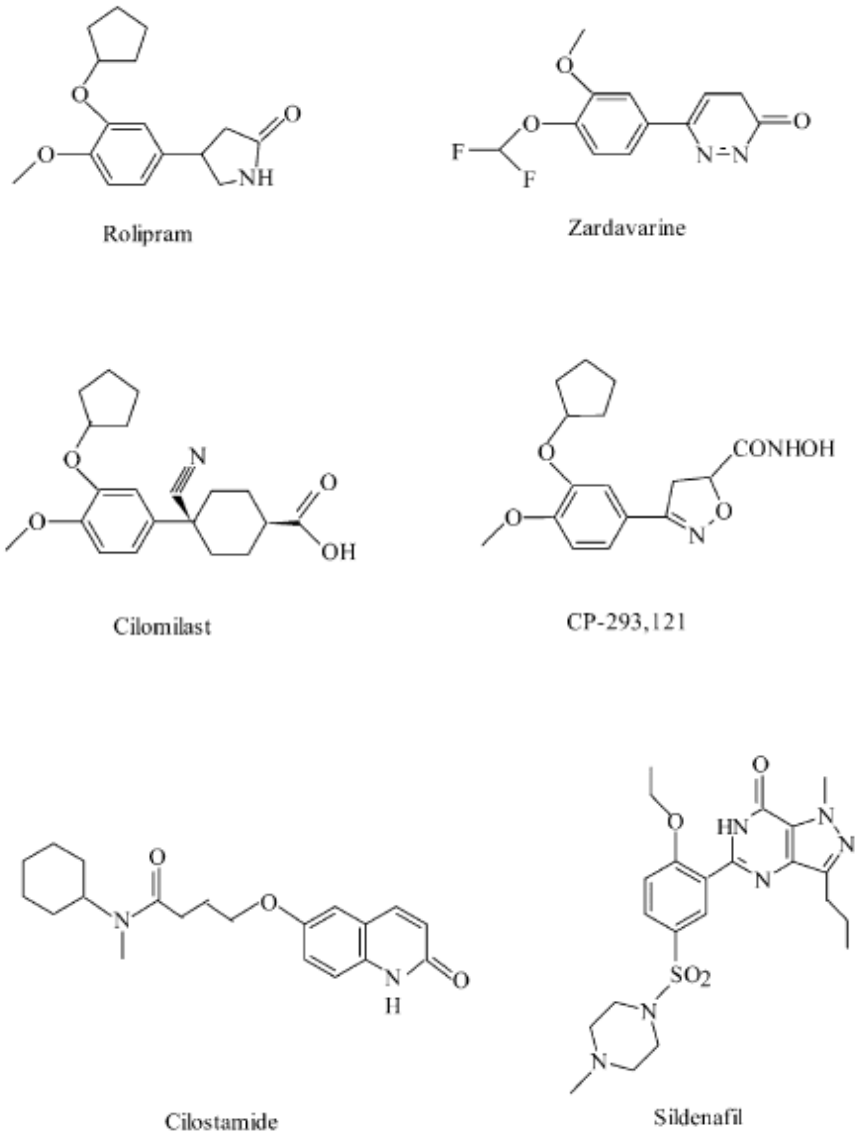


Figure 1.2. Chemical structures of the PDE Inhibitors [8]

For example, the PDE5 selective inhibitor sildenafil (Viagra; in Figure 1.2) is a drug for male erectile dysfunction, and the PDE3 selective inhibitor cilostamide is a drug for heart diseases. Zardavarine possesses selectivity for both PDE3 and PDE4 [8].

The PDE4 selective inhibitors form the largest group of inhibitors for any PDE family and have been studied as anti-inflammatory drugs targeting asthma and chronic obstructive pulmonary disease (COPD) and also as theraupetic agents for rheumatoid arthritis, multiple sclerosis, type II diabetes, septic shock, atopic dermatitis, and other autoimmune diseases [17-23]. Rolipram, cilomilast, and CP-293,121 are PDE4 selective inhibitors. The PDE4 selective inhibitor rolipram (in Figure 1.2) was studied as an antidepressant and has been used to classify the PDE families [24, 25].

## 1.2. PDE4 Gene Family and Role in Inflammation

### 1.2.1. PDE4 Isoforms

The PDE4-selective inhibitors have potential therapeutic use in a range of major disease areas so this family has attracted considerable attention over the past decade.

PDE4 enzymes specifically hydrolyze cAMP, they are widely expressed and they play major regulatory roles, as deduced from the action of highly selective inhibitors [26], targeted gene knockout [27-31], small inhibitory RNA (siRNA) ablation [32] and dominant–negative-mediated disruption of enzyme intracellular targeting [33].

They are found in many cell types and tissues such as leukocytes, airway and vascular smooth muscle, vascular endothelium and brain. The involvement of PDE4 in pathological processes associated with these tissues suggests a great potential for pharmacological intervention in a variety of inflammatory, vascular, angiogenic and neurological disorders. From the change of cAMP levels, PDE4 regulates leukocyte responses including the proinflammatory actions of monocytes, T cells and neutrophils, airway and vascular smooth muscle constriction, and neurotransmitter signaling through adenylyl cyclaselinked G-protein coupled receptors [such as that for N-methyl-D-aspartate (NMDA)]. The potential diseases for PDE4 inhibitor therapy are asthma, allergic rhinitis, atopic dermatitis, chronic obstructive pulmonary disease (COPD), rheumatoid arthritis, psoriasis, Crohn’s disease, cancer, Alzheimer’s disease, mild cognitive impairment, Parkinson’s disease, schizophrenia and depression [26,34-38].

The PDE4 gene family is composed of four genes, A, B, C, and D, each of these genes has a unique chromosomal localization and multiple splice forms of each one [39, 40]. PDE4 A and C are encoded on different regions of Chromosome 19, while PDE4 B and D are located on chromosome 1 and 5, respectively [41].

There are three groups of PDE4 isoforms:

- Long isoform
- Short isoform
- Super-short isoform (Figure 1.3) [42].

Long isoforms have two regulatory domains, the first one is the upstream conserved region 1 (UCR1) and the second one is the upstream conserved region 2 (UCR2) which is located between the isoform specific N-terminal region and the catalytic unit. The short isoforms have only UCR2 and the super-short isoforms have a truncated UCR2. A key functional role of the UCR modules is in determining PDE4 regulation through PKA and ERK phosphorylation [42, 43]. UCR1 contains a PKA phosphorylation site, allowing long isoforms to be activated by this enzyme [44, 45], thereby providing an important part of the cellular desensitization machinery for cAMP signalized by increasing the cellular capacity for cAMP degradation [45, 46]. The catalytic unit of all isoforms, except those from the PDE4A subfamily, can be phosphorylated by ERK [47-49].

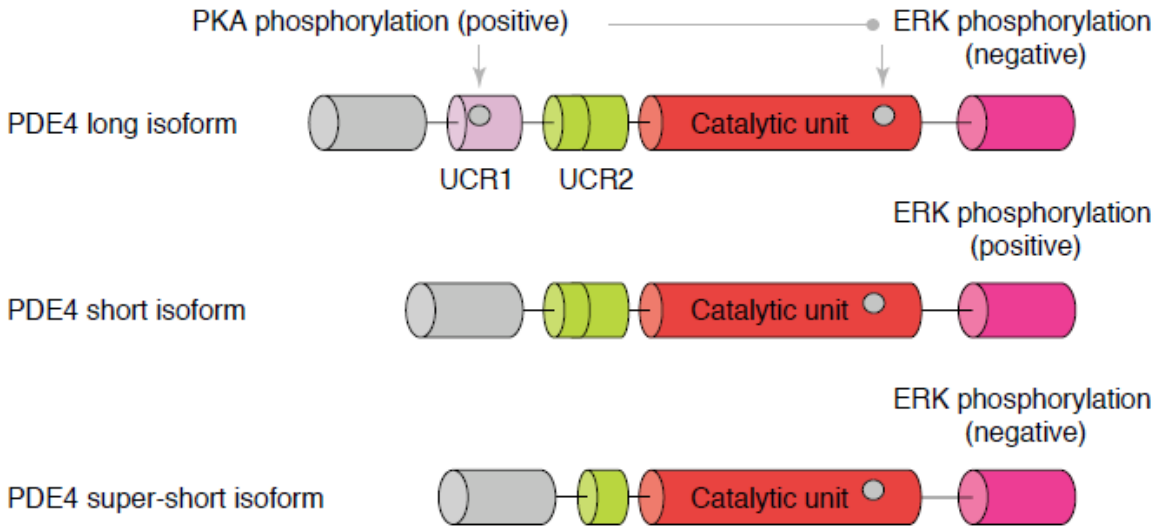


Figure 1.3. Three groups of PDE4 isoforms are defined by their unique N-terminal region. The isoform specific N-terminal region is shown in grey and the subfamily-specific C-terminal region is shown in pink [50].

### 1.3. Summary of Crystallographic Data

According to the crystal structures of PDEs that have been published up to now in Protein Databank, the overall structure of the catalytic domain of PDE enzymes can be summarized by these general points:

- PDEs are typically composed of a compact arrangement of 16 α-helices that are arranged in three subdomains: helices 1-7, helices 8-11, and helices 12-16 (Figure 1.4) [14].

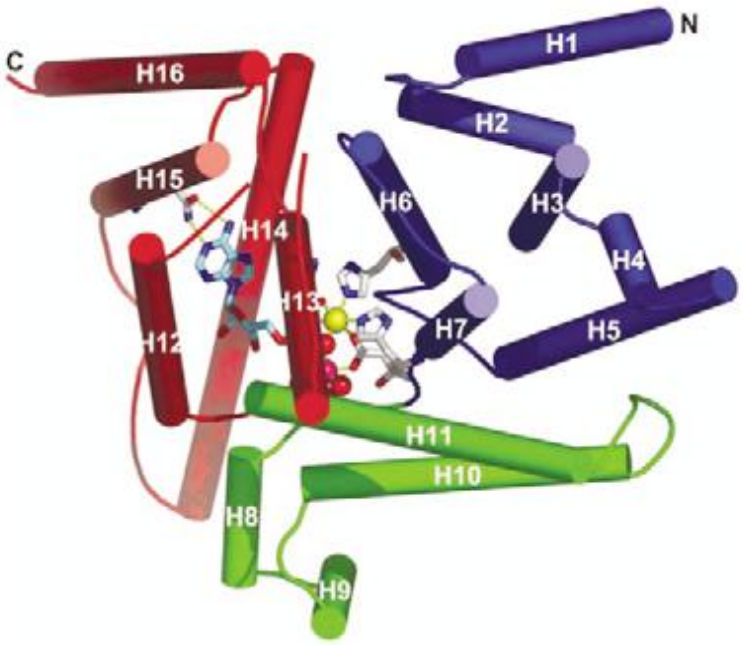


Figure 1.4. The overall structure of the catalytic domain of PDE4D.
The α-helices are represented by cylinders and the loops are represented by tubes.The α-helices labeled 1–16 are divided into three subdomains colored in blue, green and red [14].

- The active site located at the junction of the three subdomains as a deep pocket is lined with highly conserved residues. There are two divalent metal ions in the active side; Zn+2 and Mg+2. Zn2+, which is coordinated by conserved, paired histidine and aspartate residues and two water molecules, is found at the wider side of the active site. Mg2+ is also located there, coordinated by the same aspartate residue that coordinates Zn2+ as well as five water molecules (one of which bridges Mg2+ and Zn2+). This minimal interaction with protein residues shows that Mg2+ has not a structural importance. The active site pocket contains 12 of the 17 conserved residues from the 21 PDE gene family members [50]. In the active site, there are three clusters of residues which are responsible for (Figure 1.5) three important roles:

- nucleotide recognition,
- a hydrophobic clamp,
- hydrolysis.

The nucleotide recognition, where a cluster of residues determines the orientation of the amide group of an invariant glutamine residue to bind selectively either cAMP or cGMP; a hydrophobic clamp, where two highly conserved hydrophobic residues sandwich the planar purine ring involved in substrate binding; and hydrolysis, where a cluster of conserved residues near the divalent metal center are responsible for cyclic nucleotide hydrolysis [51].

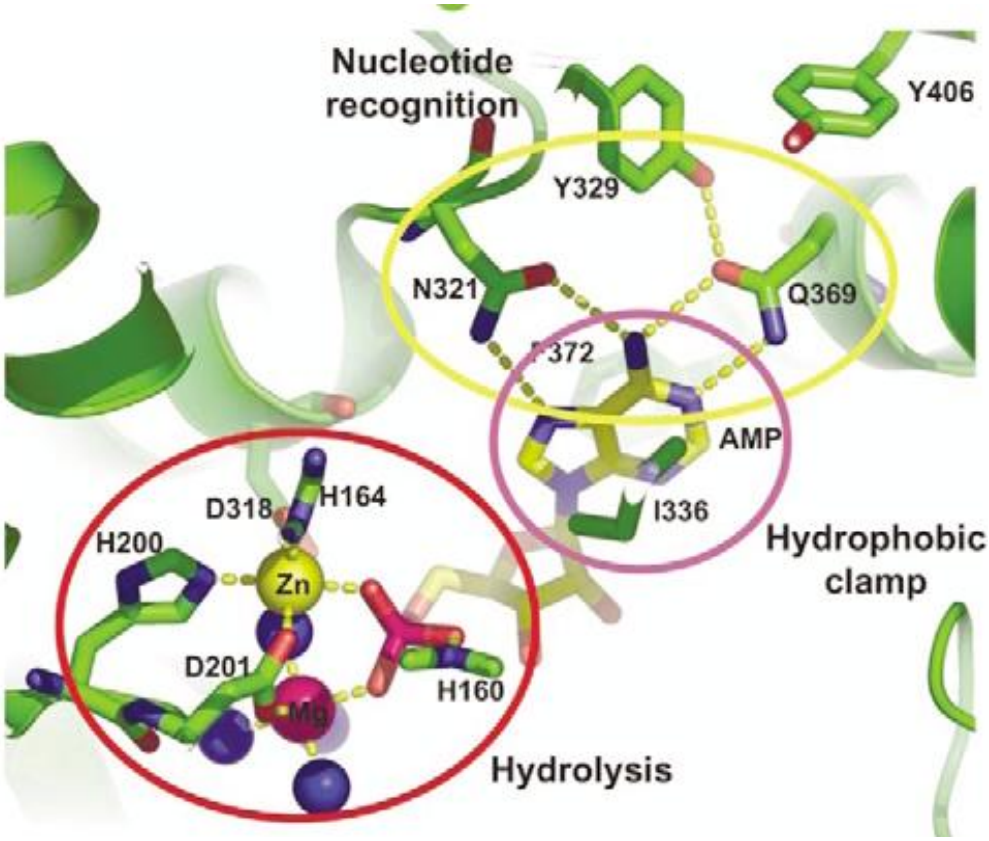


Figure 1.5. Three functional groups of residues in the active site [50]

The active site can be subdivided into three pockets (Figure 1.6) [52]:

- a metal-binding pocket (M-pocket),
- a solvent-filled side pocket (S-pocket),
- a pocket containing the purine-selective glutamine and the hydrophobic clamp (Q-pocket) [52].

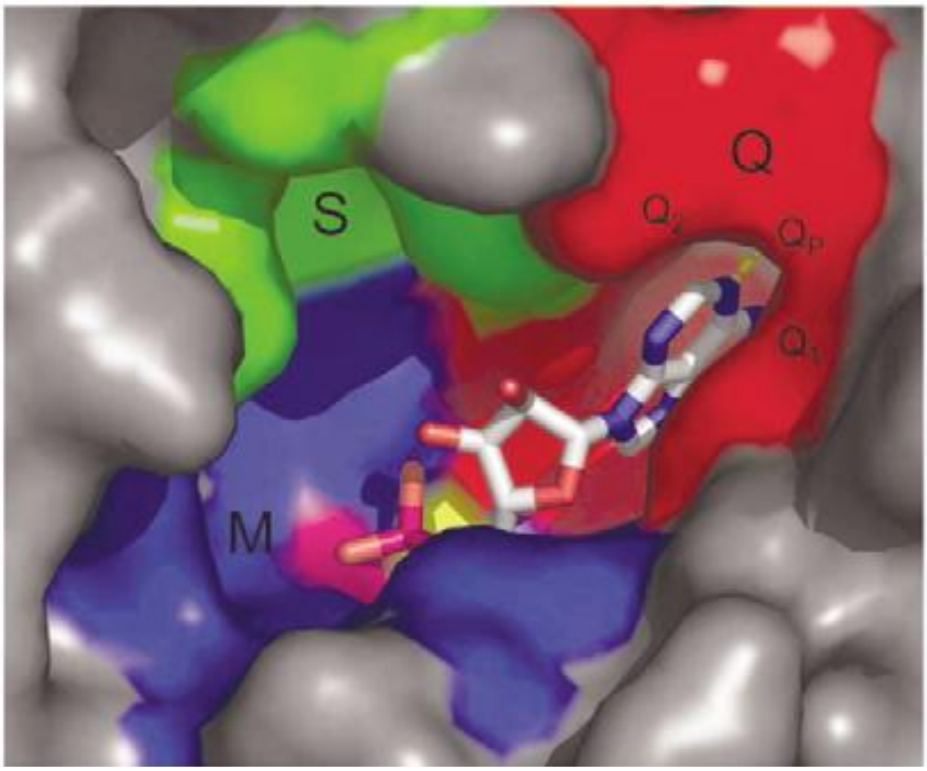


Figure 1.6. The PDE4D active site is shown with bound AMP as a stick model.The yellow and magenta surfaces are $Zn^{2+}$ and $Mg^{2+}$ ions, respectively [50].

The M-pocket contains the two divalent metal ions and highly conserved hydrophobic, polar residues that coordinate the metal ions. The S-pocket mainly includes hydrophilic amino acids and is filled with a network of water molecules in most of the inhibitor complexes. The Q-pocket can be subdivided into three distinct areas: a 'saddle' formed by the conserved glutamine and the P-clamp ($Q_P$) and two narrow, but deep, hydrophobic pockets ($Q_1$ and $Q_2$) that flank $Q_P$ [50].

### 1.4. Variety of PDE4 Inhibitor Families

Theophylline [Figure 1.7., structure (i)], although only a weak non-selective PDE inhibitor, was the first PDE inhibitor to be used therapeutically and it belongs to a family of xanthine derivatives, which also contains 3-isobutyl-1-methylxanthine (IBMX) (ii), arofylline (iii), doxofylline (iv) and cipamfylline (v). Although many xanthine derivatives have been developed, and some of them are either under clinical trials [arofylline (iii)] or

launched [doxofylline (iv)], such inhibitors are generally nonselective and relatively weak inhibitors of PDE4 [50]. Rolipram (vii) [53] has provided the paradigm for a PDE4 selective inhibitor. Many compounds have subsequently been developed, the dialkoxyphenyl (catechol) family of inhibitors being the largest and the best-characterized. Clinical trials of some of these inhibitors have been conducted for the treatment of asthma but they were hampered by dose-limiting side effects of nausea and vomiting, and therefore various strategies were undertaken to try and improve the side-effect profiles of these drugs. These include Rolipram (vii), Zardaverine (vi), Filaminast (viii), Mesopram (ix), IC-485 (xvii) and Piclamilast (xii). Others are currently in clinical trials, such as Atizoram (xv), Tetomilast (xiv), CC-1088 (xvi) and ONO-6126 (xiii). Two of the most advanced inhibitors in this catechol class, cilomilast (x) and roflumilast (xi), have completed Phase III clinical trials and they are currently waiting for regulatory approval as treatments for asthma and chronic obstructive pulmonary disease (COPD) [54]. The search for non-emetic PDE4 inhibitors has led to various, new chemical classes being developed. These include AWD-12–28 (xxii), an indole compound currently in Phase II trials for asthma; YM-976 (xxi), a pyridopyrimidinone derivative that has been discontinued after Phase I clinical trials; Tofimilast (xx), an indazole derivative in clinical development; Ibudilast (xix), a pyrazolopyridine compound that has been used extensively in the Asian market both as an asthma controller and as an eyedrop (and is also currently in Phase II clinical trials for multiple schlerosis); and Lirimilast (xviii), a benzofuran derivative that has been discontinued following a Phase II clinical trial for asthma [50].

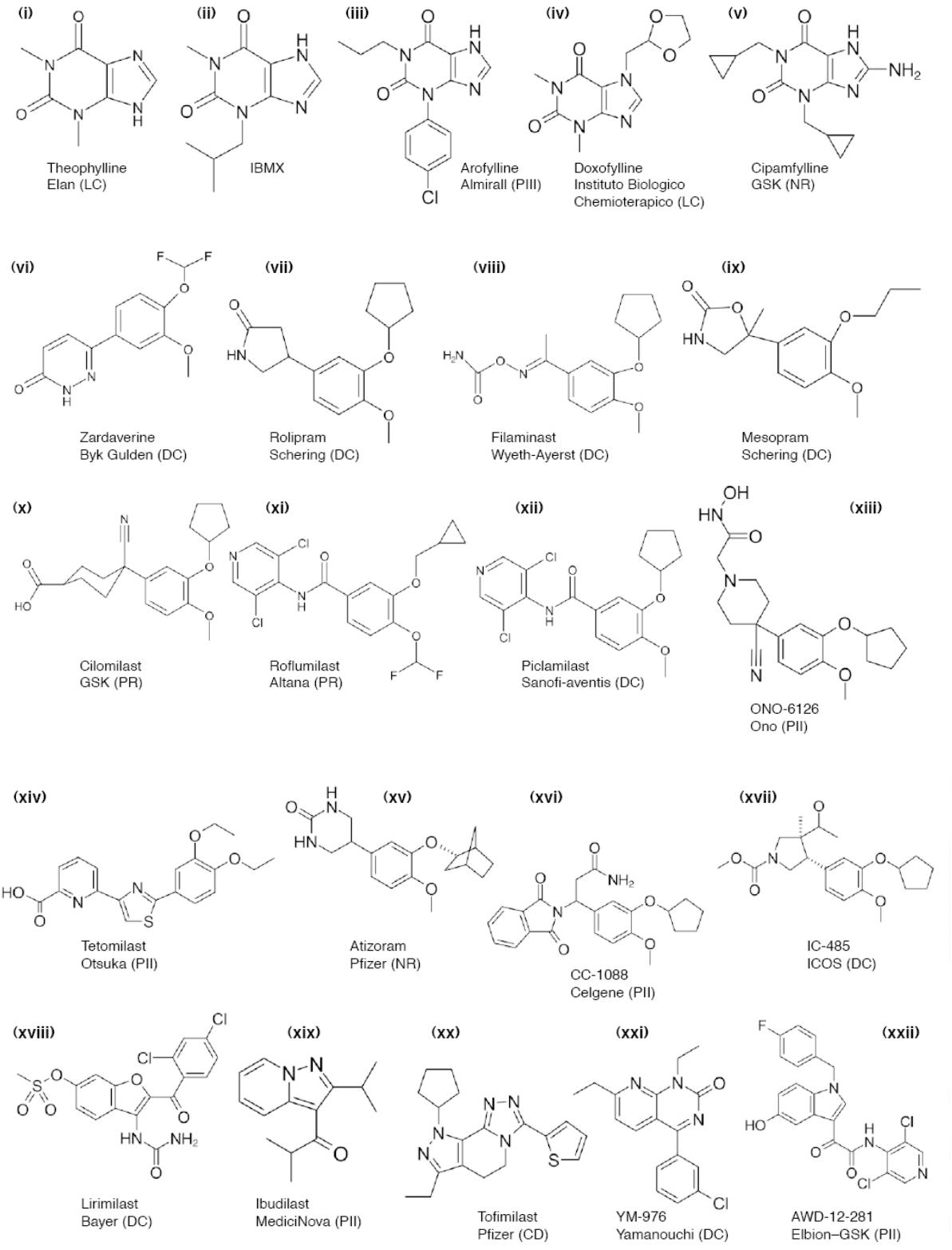


Figure 1.7. Clinical development status PDE4 inhibitors. Abbr.s: LC, launched; PR,pre-registration; PI, Phase I clinical trial; PII, Phase II clinical trial; PIII, Phase III clinical trial; CD, clinical development;DC,discontinued;NR,no development reported [50].

### 1.5. Structural Basis of Inhibitor Binding to PDE4

Structural analysis of many PDE inhibitor complexes has identified two common features of inhibitors binding to PDEs [52]. A planar ring structure of the inhibitor is held tightly in the active site by a pair of hydrophobic residues forming a hydrophobic clamp and there are H-bond interactions with the invariant glutamine residue which is essential for nucleotide selectivity [51]. These two common features define the scaffold of all known PDE inhibitors. However, interactions with residues lining the two hydrophobic subpockets that are close to the invariant purine-selective glutamine are important for inhibitor binding. Furthermore, inhibitor potency can be increased further by exploring interactions with residues near the di-metal ion center as well as through the formation of water-mediated interactions with the metal ions. There are 30 published co-crystal structures of inhibitors bound to PDE4B or PDE4D and 25 of these are unique complexes. The inhibitors represent four scaffolds: catechol, xanthani, pyrazole and purine analogs. The majority of these co-crystal structures are dialkoxyphenyl derivatives [52, 55-57] and only one is a xanthine derivative [58]. The superposition of the co-crystal structures of the dialkoxyphenyl family of compounds reveals a scaffold formed by a catechol, H-bonding to the purine-selective glutamine, which is surrounded by the P-clamp. The catechol scaffold superposes extremely well in all of these co-crystal structures, whereas the substituents show significant variations in their binding conformation as well as in the residues that they interact with. The various substituents on the catechol scaffold explore the deep pocket close to the metal binding site and their ability to form interactions with residues lining this pocket determines their relative binding affinity. The relatively smaller pyrrolidinone substituent in rolipram resulted in a relatively lower binding affinity that is similar to that reported for PDE4B as a low-affinity conformer [59]. Both *R*-rolipram and the racemic (*R*–*S*)-rolipram adopt a single binding conformation in PDE4B and PDE4D [52, 57]. However, two binding conformations for (*R*–*S*)-rolipram have been observed in one study [56] supporting the notion that PDE4 enzymes can adopt distinct conformations. Notwithstanding this, the true conformation that PDE4 adopts when it binds rolipram with heightened affinity has yet to be unequivocally demonstrated. The more potent dialkoxyphenyl compounds have larger substituents that form more favorable interactions with residues lining the relatively large M-pocket. The most potent compounds, such as roflumilast and piclamilast, reach deep into the M-pocket, not only interacting with

residues near the metal ion but also forming H-bonds with a water molecule that is coordinated to the metal ion. Surprisingly, none of the inhibitors (with the exception of zardaverine) interact directly with the metal ions [50].

## 1.6 Aim of The Study

The primary aim of this study is to carry out molecular docking process of novel inhibitors for Phosphodiesterase4 (PDE4) enzyme.

Virtual screening and 3D pharmacophore models will be used before the docking process for Phosphodiesterase4 (PDE4) inhibitors

# 2. THEORY

## 2.1 Virtual Screening

Virtual screening is the computational or in silico analogue of biological screening. The aim of virtual screening is to score, rank or filter a set of structures using one or more computational procedures [60].

Virtual screening is used, for example, to help decide which compounds to screen, which libraries to synthesize and which compounds to purchase from an external company. It may also be employed when analyzing the results of an experiment, such as a high-throughput screening (HTS) run [60].

There are many different criteria by which the structures may be scored, filtered, or otherwise assessed in a virtual screening experiment. For example, one may use a derived mathematical model such as a multiple linear regression equation to predict the biological activity of each structure. One may use a series of substructure queries to eliminate molecules that contain certain undesirable functionalities. If the structure of the target protein is known, one may use a docking program to identify structures that are predicted to bind strongly to the protein active site [60].

The number of structures that may need to be considered in virtual screening experiments can be very large; when evaluating virtual combinatorial libraries the numbers may run into the billions. It is therefore important that the computational techniques used for the virtual screening have the necessary throughput. This is why it may often be most effective to use a succession of virtual screening methods of increasing complexity [61]. Each method acts as a filter to remove structures of no further interest, until at the end of the process a series of candidate structures are available for final selection, synthesis or purchase [60].

Wilton et al. [62] have suggested that there are four main classes of virtual screening methods, according to the amount of structural and bioactivity data available.

If just a single active molecule is known then similarity searching can be performed in what is sometimes known as ligand-based virtual screening. If several active molecules are available then it may be possible to identify a common 3D pharmacophore, followed by a 3D database search. If a reasonable number of active and inactive structures are known they can be used to train a machine learning technique such as a neural network which can then be used for virtual screening. Finally, protein–ligand docking can be employed when the 3D structure of the protein is known. In addition to these methods that are specific to particular targets, virtual screening techniques have been developed that are of more general applicability. These include, for example, methods that attempt to predict the likelihood that a molecule possesses "drug-like" characteristics and that it has the desired physiochemical properties to be able to reach its site of action within the body. A schematic illustration of a typical virtual screening flowchart is shown in Figure 2.1 [60].

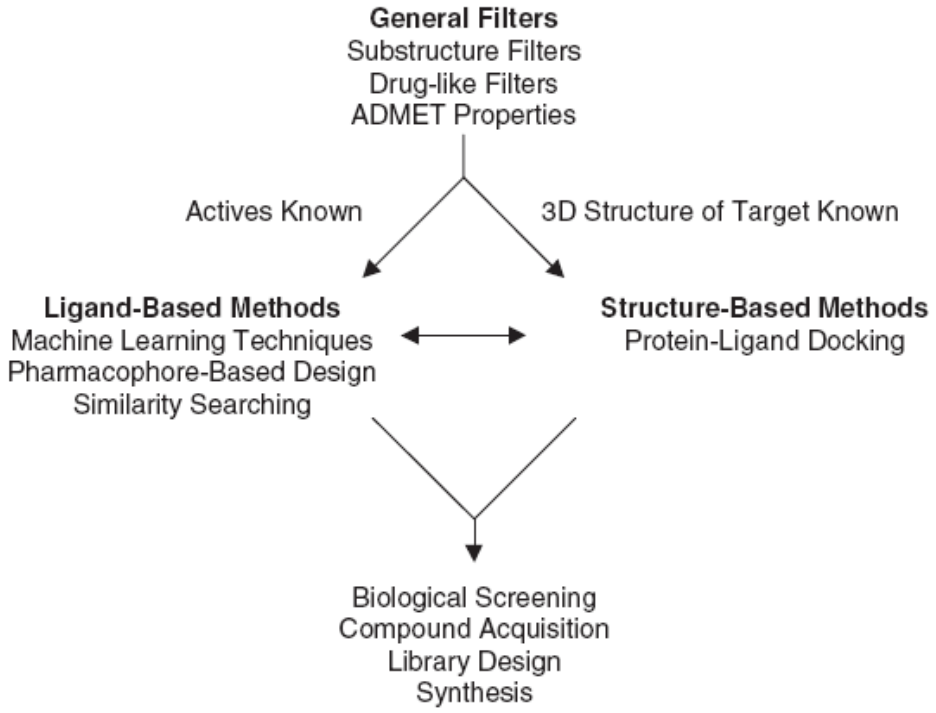


Figure 2.1. Many virtual screening processes involve a sequence of methodologies [60].

## 2.2. 3D Pharmacophores

A 3D pharmacophore is usually defined as a set of features together with their relative spatial orientation. Typical features include hydrogen bond donors and acceptors, positively and negatively charged groups, hydrophobic regions and aromatic rings. The use of such features is a natural extension of the concept of *bioisosterism*, which recognizes that certain functional groups have similar biological, chemical and physical properties [63].

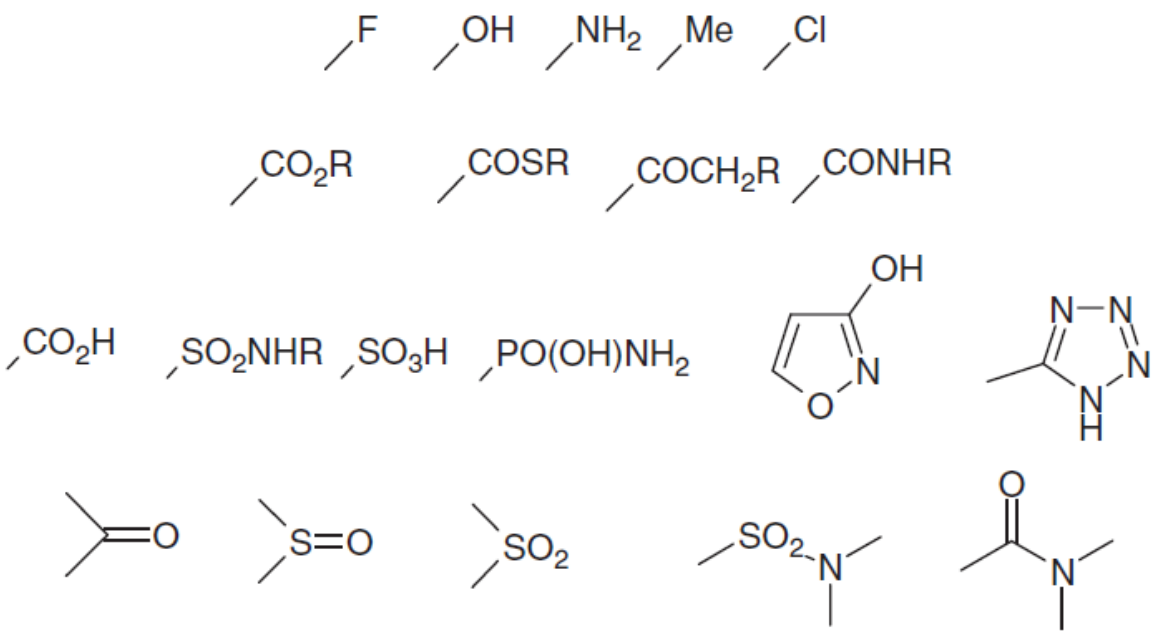


Figure 2.2. A selection of common bioisosteres; each line contains a set of distinct functional groups [60].

Many authors use the term "pharmacophores" to define functional or structural elements possessing biological activity [64]. This does not correspond to the official definition elaborated by an IUPAC working party and published in 1998 [65]: *A pharmacophore is the ensemble of steric and electronic features that is necessary to ensure the optimal supramolecular interactions with a specific biological target structure and to trigger (or to block) its biological response.* As a consequence:

i. The pharmacophore describes the essential, steric and electronic, function-determining points necessary for an optimal interaction with a relevant pharmacological target.

ii. The pharmacophore does not represent a real molecule or a real association of functional groups, but a purely abstract concept that accounts for the common molecular interaction capacities of a group of compounds towards their target structure.

iii. Pharmacophores are not specific functional groups (e.g. sulfonamides) or “pieces of molecules” (e.g. dihydropyridines, arylpiperazines) [64].

A pharmacophore can be considered as the highest common denominator of a group of molecules exhibiting a similar pharmacological profile and which are recognized by the same site of the target protein [64].

### 2.2.1. Methods To Derive 3D Pharmacophores

How can 3D pharmacophores be determined? Traditionally, 3D pharmacophore approaches are used when active molecules are known but where the structure of the target receptor is not available. The process of deriving a 3D pharmacophore is called pharmacophore mapping. There are two key issues to consider when deriving 3D pharmacophores. The first issue concerns the conformational flexibility of the molecules and how to take this into account. The second problem concerns the fact that there may be many different combinations of pharmacophoric groups within the molecules. As a consequence, there may be hundreds of potential 3D pharmacophores. The objective is to determine which of these potential pharmacophores best fits the data. In general, the aim is to identify the 3D pharmacophore(s) that contains the largest number of features common to all of the active molecules, and where these common features can be presented by each molecule in a low-energy conformation. Note that the generation and use of 3D pharmacophores is therefore based upon the assumption that all of the molecules bind in a common manner to the biological target [60].

Various methods have been devised for performing pharmacophore mapping: constrained systematic search, clique detection, the maximum likelihood method and the Genetic Algorithm (GA) approach [60].

### 2.2.2. Criteria for a Satisfactory Pharmacophore Model [66]

To be recognized as a useful tool, a pharmacophore model has to provide valid information for the medicinal chemist exploring structure–activity relationships.

- First, it has to highlight the functional groups involved in the interaction with the target, the nature of the non-covalent bonding and the different intercharge distances. This means that worthless images of ribbon and spaghetti models [67], without indication of the molecular features of the interacting partners, have to be avoided. This is true also for many unnecessary and opaque theoretical digressions. The model also has to show some predictive power and lead to the design of new, more potent compounds or, even better, of totally novel chemical structures, not evidently deriving from the translation of structural elements from one active series into the other. An interesting aspect of pharmacophore-based analogue design is referred to as scaffold hopping. It consists in the design of functional analogues by searching within large virtual compound libraries of isofunctional structures, but based on a different scaffold. The objective is to escape from a patented chemical class in identifying molecules in which the central scaffold is changed but the essential function-determining points are preserved and form the basis of a relevant pharmacophore [68].

- The second criterion for a valid pharmacophore model is that it should discriminate stereoisomers. Stereospecificity is one of the principal attributes of pharmacological receptors and a perfect stereochemical complementarity between the ligand and the binding-site protein is an essential criterion for high affinity and selectivity. A convincing example of enantiomeric discrimination was observed for GABA-A receptor antagonists [68].

- In a similar manner, the ideal model should distinguish between agonists and antagonists. This is relatively easy for the specific category of antagonists which,

according to Ariëns et al. theory [69], derive from the agonists simply through the addition of some supplementary aromatic rings which play the role of additional binding sites (e.g. the passage from muscarinic agonists to muscarinic antagonists [70] or from GABA agonists to GABA antagonists [68]). The discrimination between the two categories becomes less evident when the passage from agonist to antagonist relies on relatively subtle changes such as one observes for glutamate, oxotremorine and benzodiazepine antagonists.

- Sometimes a good pharmacophore model can *explain* apparently *paradoxical observations,* e.g. the unexpected affinity reversal found in *R*- and *S*-enantiomers of the sulpiride series on changing *N*-ethyl to *N*-benzyl derivatives [71].

- Finally, it has to account for the *lack of activity* of certain analogues of the active structures. The knowledge of structural or electronic parameters leading to poorly active or inactive compounds is a cost-lowering factor that allows the number of compounds to be synthesized to be reduced [64].

### 2.3. Drug Likeness and Compound Filters

Among the simplest types of methods that can be used to assess "druglikeness" are substructure filters [60]. A compound collection may include molecules that contain reactive groups known to interact in a nonspecific manner with biological targets, molecules that give "false positive" results due to interference with certain types of biological assay, or molecules which are simply inappropriate starting points for a drug discovery programme [72]. Many of these features can be defined as substructures or as substructure counts that are used to filter both real and virtual data sets. One may wish to apply such filters to the output from a high-throughput screening (HTS) run, in order to eliminate known problem molecules from further consideration (of course, one would prefer to eliminate such compounds prior to the screen). They are also extremely useful when designing virtual libraries and when selecting compounds to purchase from external suppliers. One should, however, always remember that such filters tend to be rather general in nature and that for any specific target it may be necessary to modify or extend them accordingly [60].

Other approaches to the question of "drug-likeness" were derived by analyzing the values of relatively simple properties such as molecular weight, the number of rotatable bonds and the calculated logP in known drug molecules. Considerations such as these led to the formulation of the "rule of five" [73] which constitutes a set of simple filters that suggest whether or not a molecule is likely to be poorly absorbed. The "rule of five" states that poor absorption or permeation is more likely when:

- The molecular weight is greater than 500,
- The log*P* is greater than five,
- There are more than five hydrogen bond donors (defined as the sum of OH and NH groups),
- There are more than ten hydrogen bond acceptors (defined as the number of N and O atoms),
- There are more than eight rotatable bonds.

Excluded from this definition are those compounds that are substrates for biological transporters. An obvious attraction of this model is that it is extremely simple to implement and very fast to compute; many implementations report the number of rules that are violated, flagging or rejecting molecules that fail two or more of the criteria. A more extensive evaluation of property distributions for a set of drugs and non-drugs has identified the most likely values for "drug-like" molecules [74]. For example, 70% of the "drug-like" compounds had between zero and two hydrogen bond donors, between two and nine hydrogen bond acceptors, between two and eight rotatable bonds and between one and four rings. The "rule of five" was derived following a statistical analysis of known drugs; a similar analysis has since been carried out on agrochemicals with modified sets of rules being derived that relate to the properties of herbicides and insecticides [75].

## 2.4. Structure-Based Virtual Screening

As the number of protein crystal structures has increased so too has the interest in using this detailed structural knowledge for library design, compound acquisition and data analysis. Structure-based design methods have been developed over many years. However, much of this activity was geared towards methods for the detailed analysis of small

numbers of molecules. Several factors have contributed to the move towards higher-throughput structure-based methods. First, high-performance computer hardware (often based on the linux operating system) has provided unparalleled amounts of dedicated computing power at a low cost to researchers. Second a significant effort has been expended in the development of new algorithms, particularly for molecular docking. Finally, tools for the analysis of the output of such calculations enable scientists to navigate more effectively through the large quantities of data generated [60]

## 2.5. Protein-Ligand Docking

Docking is an automated computer algorithm that determines how a compound will bind in the active site of a protein. This includes determining the orientation of the compound, its conformational geometry, and the scoring. The scoring may be a binding energy, free energy, or a qualitative numerical measure. In some way, every docking algorithm automatically tries to put the compound in many different orientations and conformations in the active site, and then computes a score for each. Some programs store the data for all of the tested orientations, but most only keep a number of those with best scores. Docking functionality is built into full-featured drug design programs, and sold as stand-alone programs, sometimes with their own graphical interface [76].

Docking is probably the most heavily used tool in computational drug design. It is also the most accurate method for predicting whether a particular compound will be a good inhibitor of a particular protein. For this reason, pharmaceutical companies analyze very large numbers of compounds with docking. Those compounds that have the best docking results will be synthesized if necessary, and analyzed in the laboratory. The large lists of compounds that are analyzed computationally may be of compounds designed in the computer, compounds that are available for purchase, or compounds in the company compound library. By using the knowledge gained from the docking study, fewer compounds need be synthesized and assayed are found to be active [76].

Because docking calculations simulate the interaction between a compound and a protein’s active site, the results are comparable to those of biochemical assays. Most scoring functions compute some sort of energy. Most biochemical assays compute an

inhibition rate constant $K_i$. Thus, the binding energy from the docking calculation should be proportional to ln $K_i$ from biochemical assays( a simple Arrhenius eqation relationship). Some scoring functions show good correlation to ln $K_i$, while others give only a qualitative ranking showing which compound are better or worse [76].

The primary reasons for using docking are to predict which compounds will bind well to a protein, and to see the three-dimensional geometry of the compound bound in the protein's active site. One limitation of docking is that a 3D structure of the target protein must be available. Also, the amount of computer time required to run docking calculations is not insignificant. Thus, it may not be practical to use docking to analyze very large collections of compounds. Less CPU-intensive techniques, such as pharmacophore or similarity searches, can be used to search very large databases for potentially active compounds. Compounds identified by those techniques are often subsequently run through a docking ananlysis. Pharmacophore searches are used to search databases of millions of compounds. Docking might be used to analyze tens or hundereds of thousands of compounds over the course of a multiyear drug design project [76].

## 2.6. The Docking Process

### 2.6.1. Protein Preparation

The accuracy of docking results is directly related to the quality of the crystallographic structure for the protein's active site. If the enzyme requires a cofactor, then the crystallographic structure of the haloenzyme (with the cofactor attached) should be used. Since even the best crystallographic structures often have a resolution of the order of 1Å or more, most researches will start with the crystallographic structure with an inhibitor in the active site, and then add the hydrogens that cannot usually be seen by protein crystallography. Water molecules are removed, sometimes with the exception of structural waters in the interior of the protein. Finally, a simple minimization is performed to find the nearest minimized structure, as predicted by the force field being used. This minimized structure is often the best structure to utilize for docking studies, particularly if the crystallographic resolution was marginal [76].

### 2.6.2. Building the Ligand

Docking programs offer several options for creating ligands and placing them in the active site. At the most automated end of spectrum, some docking programs can take a database of ligands, place each one in the active site, and do the docking run. This completely automated approach allows thousands of compounds to be analyzed without manual intervention from the user. Some docking programs are slightly less automated in that they automatically dock a list of ligands from a database, but each ligand must be stored in the database with its position, orientation, and conformation set within the coordinate system to put the initial placement in the protein's active site [76].

### 2.6.3. Setting the Bounding Box

The entire protein is read into the computer in order to obtain a correct geometry for the structure. However, docking calculations can take a significant amount of time, and anything that speeds them up without loss of accuracy is utilized. Protein residues far from the active site do not generally have any measurable effect on the scoring results. In order to speed the calculation, a cutoff distance is set, and no interactions are computed for residues beyond that distance from the ligand. For ease of coding, this cutoff is usually a rectangular box, called a bounding box. In the case of grid poteintials, the grid is only computed for points within the cutoff distance. Many docking packages default to setting the bounding box far enough out from the ligand or active site that there is no need to alter it. However (at least when starting on a set of docking runs), the user should verify that the bounding box extends a reasonable distance beyond the active site in all directions [76].

### 2.6.4. Docking Options

When setting up the inputs to a docking calculation, there will be options for flexible active sites, scoring method, search method, solvation, handling encapsulated active sites, etc. Some packages may have an option to do a fast initial check, and then continue only if the first check criterion satisified. Nearly always, the docking results will be more accurate with the calculation running more slowly, if an optimization (or at least a few optimization steps) is performed for each pose [76].

### 2.6.5. Running the Docking Calculation

Once the inputs have been set, the docking calculation can be run. Most docking programs allow individual docking runs to be started from the graphical interface. A few docking programs can run many docking calculations in a batch mode. These calculations are sometimes run on the same computer where the graphical interface is used, and sometimes can be sent off to a different server [76].

### 2.6.6. Analysis of Results

The most important result from a docking calculation is the binding energy of the ligand to the active site. This is the value that is compared between different compounds to determine which will be the best inhibitor. The pose of the ligand in the active site associated with a few of the best binding energies is examined visually to ensure that it looks reasonable. Sometimes, the pose generated by one docking calculation gives the researcher an idea on how to alter the compound on the next round of calculations [76].

### 2.6.7. Validation of Results

When a docking study begins, the choice of docking and scoring algorithms should be validated for that particular protein with ligands as similar as practical to those to be studied. Because scoring energies are used for compound selection in the drug design process, it is most important to make sure that the scoring energy is sufficiently accurate. This is done by comparing docking energies with biochemical assay results. Since the most biochemical assays yield inhibition rate constants, this means making sure that the docking energy is proportional to ln $K_i$.

Even with the best docking programs in existence, there will be not be a perfect correlation between docking energy and ln $K_i$. However, this is the most valid comparion between docking and experimental results, making it the best criterion for suggesting which docking program is best for a particular study. The correlation coefficient and graph from a validation study are a good indication of how much, or how little, accuracy to expect from the docking simulation. The docking experiments will rank compounds by

predicted activity, but, as indicated by correlation coefficients, it is more correct to start with the docking energy and bin out the top 50 compounds, the next 50, and so on.

The geometry of the ligand binding conformation can also be compared with experimental results. This is done by comparing with crysallographic data. Often, a root mean square deviation (RMSD) between the computational and experimental results is presented. Unless a method gives a glaringly bad RMSD, researches are encouraged to use this as only a very small factor in choosing a docking code. In general, methods that give accurate energies also give accurate geometries [76].

# 3. METHODOLOGY

In this study, the pharmacophore models were prepared by using LigandScout [80] software package and the chosen model was improved with Catalyst program.

Virtual screening was carried out with 6 databases and the docking process was completed with AutoDock 4.0 [81] (see Appendix B).

After the docking process, the best pose of ligands is taken and the single-point energies are calculated with Spartan 04 package. The most stable conformers of the hit molecules were found by carrying out a conformer search using the semi-empirical PM3 method by using the Spartan 04 program package.

The strain energy was calculated as the difference between the best pose of ligands after the docking process with AutoDock 4.0 [81] and the optimized conformation of ligands with semi-emprical PM3 method by using the Spartan 04.

## 3.1. Pharmacophores from Macromolecular Complexes with LigandScout [80]

LigandScout is a software tool that allows to rapidly and transparently derive 3D pharmacophores from structural data of macromolecule/ligand complexes in a fully automated and convenient way [80].

LigandScout deals with data mining in protein complexes that have been continuously submitted for over 30 years. The file format used was mainly created to describe proteins, never focusing on ligands or their detailed description. In order to yield the best results from data gathering, a potential interpretation algorithm needs to eliminate any possible means of data tampering caused by automated conversion. This is the reason why this work has to perform interpretation starting from the slightly outdated original PDB file format, which was used to submit the largest part of all ligands complexed in proteins [80].

LigandScout pharmacophores solely consist of chemical features classified as layers 3 and 4 according to a  a simple layer model in order to describe the levels of universality and specificity of chemical features.

- Layer 1: A phenol group facing a parallel benzenoid system within a distance of 2–4 Å.
- Layer 2: A phenol group.
- Layer 3: H-bond acceptor vector including an acceptor point as well as a projected donor point; aromatic ring including a ring plane.
- Layer 4: H-bond acceptor without the projected point; lipophilic group.

Visualization mainly distinguishes between point and vector features: point features (layer 4) are defined as a center with a tolerance; this group encompasses hydrophobic, positively ionizable and negatively ionizable areas, in addition to excluded volume spheres. Hydrogen donors, acceptors and donor–acceptor pairs belong to the vector features group. Point features are rendered as spheres with different colors to differentiate them (Fig. 3.1.): hydrophobic/lipophilic features are drawn in yellow and positive and negative ionizable features are drawn in red and blue, respectively. Excluded volume spheres use a dark gray color to signify their meaning. Spheres are drawn as semi-transparent objects, with a wire frame on their surface to enhance the impression of depth and to make it easier to judge the size of the spheres in the third dimension [64].

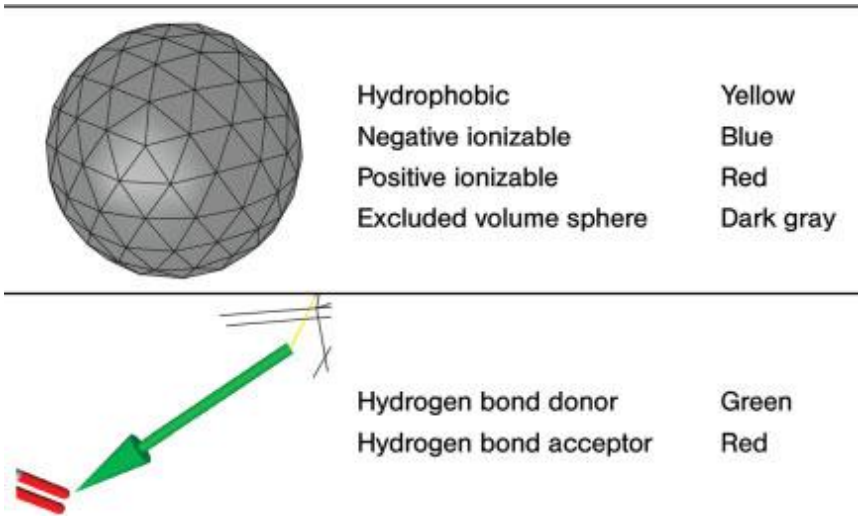


Figure 3.1. Different features in the pharmacophore visualization [64].

### 3.2. Docking with AutoDock

AutoDock is a suite of docking tools developed at The Scripps Research Institute [81] (http://autodock.scripps.edu/). It is designed to predict how small molecules, such as substrates or drug candidates, bind to a receptor of known 3D structure [76].

AutoDock actually consists of two main programs: AutoDock performs the docking of the ligand to a set of grids describing the target protein and AutoGrid pre-calculates these grids.

In addition to using them for docking, the atomic affinity grids can be visualised. This can help, for example, to guide organic synthetic chemists design better binders.

Also a graphical user interface called AutoDockTools, or ADT for short, which amongst other things helps to set up which bonds will treated as rotatable in the ligand and to analyze dockings.

For the AutoDock 4.0, detailed information can be found in Appendix A.

# 4. RESULTS AND DISCUSSION

As mentioned before, the potentially important clinical benefits of PDE4 inhibition, coupled with the limitations of current PDE4 inhibitors, highlight the need for novel PDE4 inhibitor chemotypes. Furthermore mutations in the enzyme deactivate the enzyme, thus it is quite important to design new potent ligands for PDE4.

In this study, computational tools will be used to design new ligands to inhibit the enzyme PDE4. The X-ray structure of PDE4 complexed with rolipram will be first considered, rolipram will be removed from the active site, virtual compound libraries for PDE4 will be screened for ligands which will be docked into the active site of PDE4. The docking results will be used to filter the candidate molecules. Finally the internal energy of the best docked pose of selected compound will be compared to the internal energy of the best conformation of selected compounds. The energy differences will be used to estimate the conformational strain energy of the docked pose .

## 4.1. Pharmacophore Models

In this study, the first job was to search the phosphodiesterase 4 enzyme in the Protein Databank and 44 X-ray crystal structures were found. The 44 X-ray crystal structures are encoded by 4 distinct genes A, B, C, and D. It was wanted to find novel inhibitors selective for only 1 subtype of these genes. According to the literature search, it was understood that finding a selective inhibitor for either A or C is not probable so we eliminated the X-ray crystal structures which came from A and C genes and focused on the B and D subtypes.

After that, for pharmacophore models, 4 different X-ray crystal structures were chosen:

- 1RO6 PDE4B crystal structure with ligand rolipram
- 1XM4 PDE4B crystal structure with ligand piclamilast

- 1Y2J PDE4B crystal structure with ligand 3,5-Dimethyl-1-(3-Nitro-Phenyl)-1H-Pyrazole-4-Carboxylic Acid Ethyl Ester
- 2FM0 PDE4D crystal structure with ligand L-869298

The pharmacophore models were prepared with LigandScout software in the Computer-aided Molecular Desing Group, supervised by Dipl.-Ing. Dr. Gerhard Wolber and Dott.ssa Simona Distinto, at the Computational Work, Department of Pharmaceutical Chemistry at the Institute of Pharmacy of the Leopold-Franzens-University of Innsbruck, Austria.

The first pharmacophore was modeled according to 1RO6 X-ray crystal structure (Figure 4.1. ).

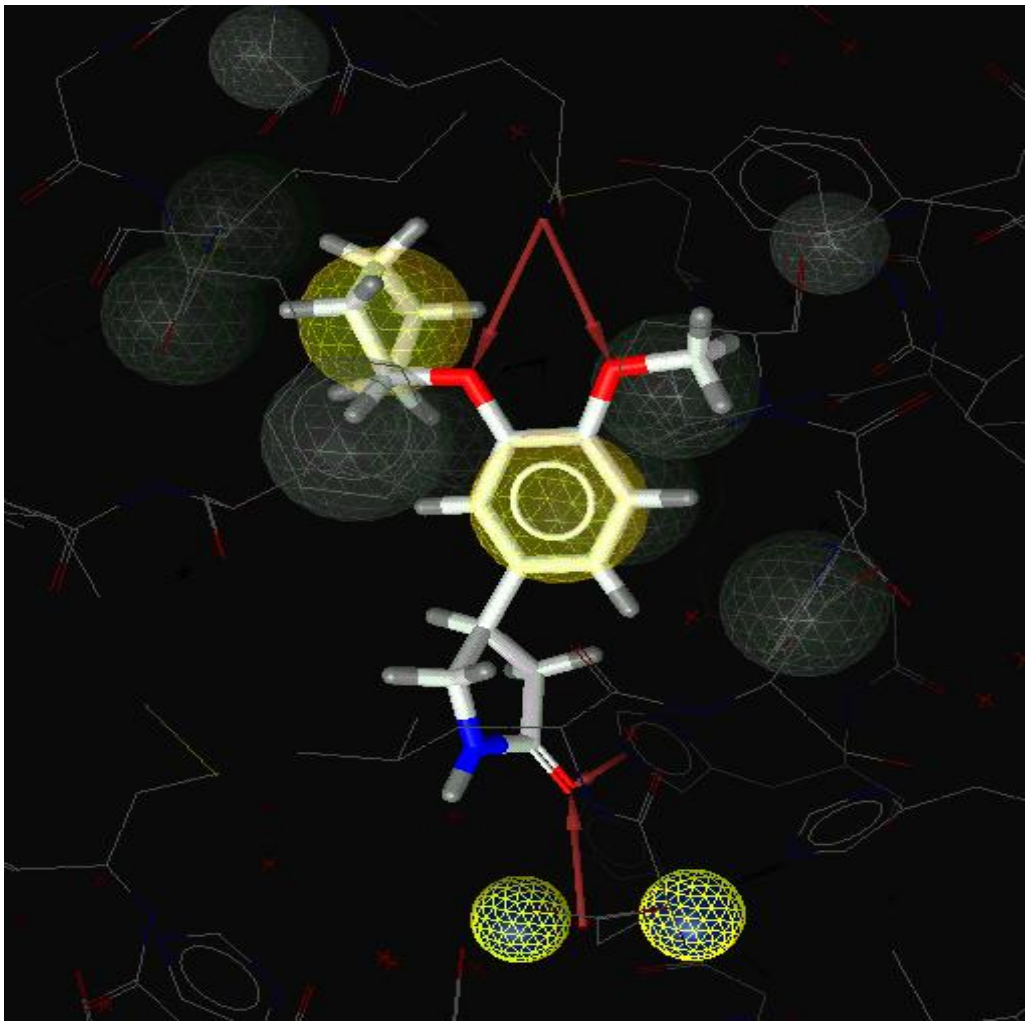

Figure 4.1. 1RO6 pharmacophore model prepared with LigandScout program

In the first model (Figure 4.1. ), the natural ligand of 1RO6 X-ray crystal structure is rolipram. There is a feature on the aromatic ring and also on the five-membered ring at the top portion of the rolipram. At the top portion, the oxygen atom can give a good interaction with the GLN 443A residue and at the bottom part, the carbonyl oxygen on the five-memered ring can interact with the water molecule ($H_2O$ 788A residue) between 2 divalent metal ions, $Zn^{+2}$ and $Mg^{+2}$.

The second model was prepared according to the 1XM4 X-ray crystal structure (Figure 4.2).

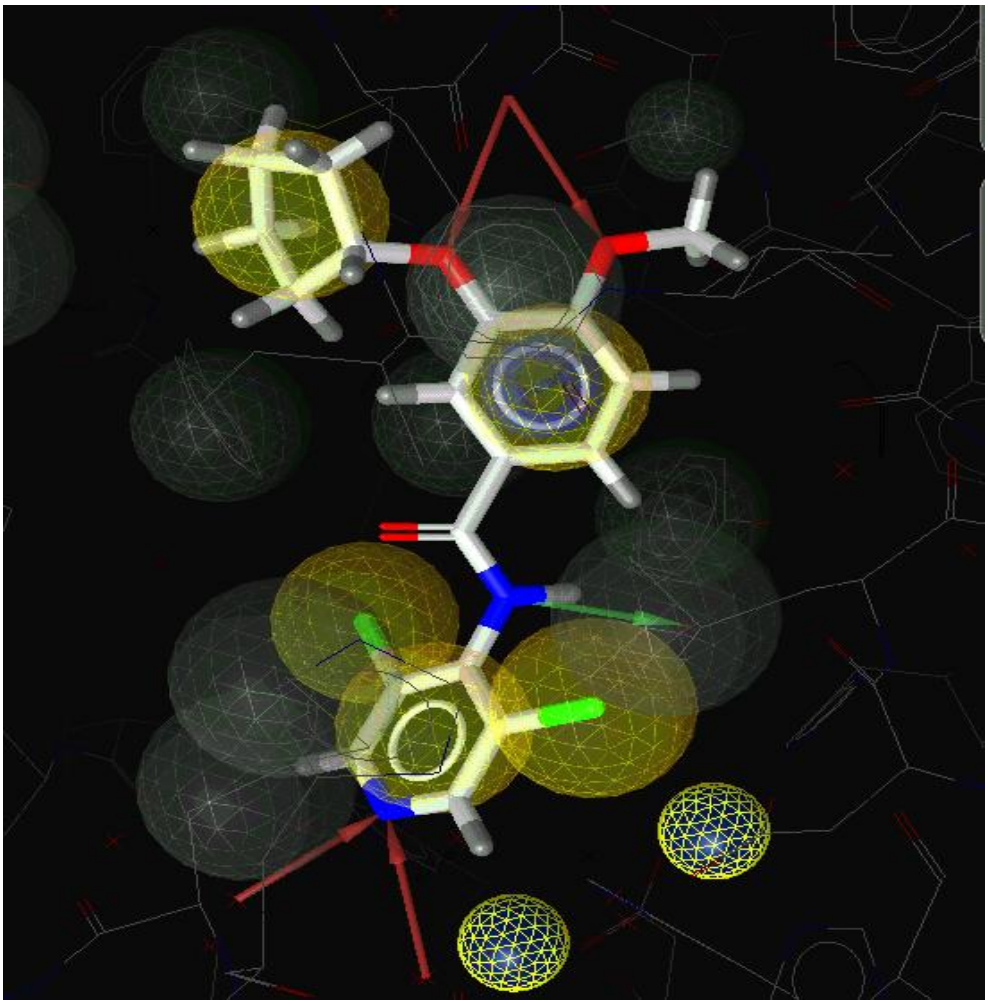

Figure 4.2. 1XM4 pharmacophore model prepared with LigandScout program

In the second model (Figure 4.2), the natural ligand is piclomilast. Again there is an aromatic feature on the aromatic ring. We can see an essential interaction between GLN 443A residue and the oxygen atom at the top portion of the molecule. Also the nitrogen atom on the six-membered ring can give interactions with residues at the bottom portion of the molecule.

1Y2J is the third pharmacophore model which was prepared with LigandScout program (Figure 4.3).

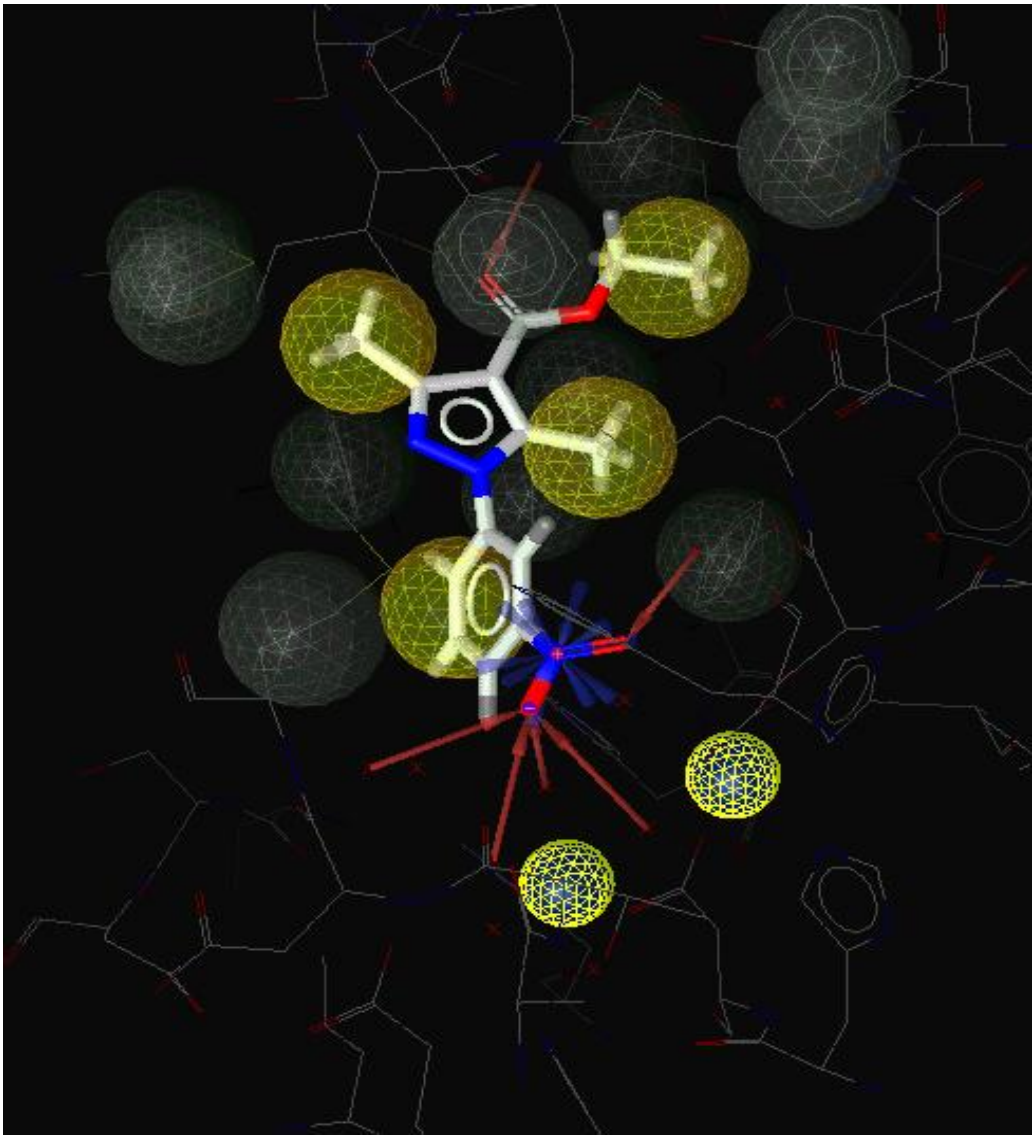

Figure 4.3. 1Y2J pharmacophore model prepared with LigandScout

In the third model (Figure 4.3), 3,5-Dimethyl-1-(3-Nitro-Phenyl)-1H-Pyrazole-4-Carboxylic Acid Ethyl Ester is the natural ligand. The aromatic ring feature is same as the other 2 models and the oxygen which is bonded to the nitrogen can interact with the water molecule ($H_20$ 788A residue) between the 2 divalent metal ions, $Zn^{+2}$ and $Mg^{+2}$.

2FM0 is the fourth pharmacophore which was modeled with LigandScout program (Figure 4.4)

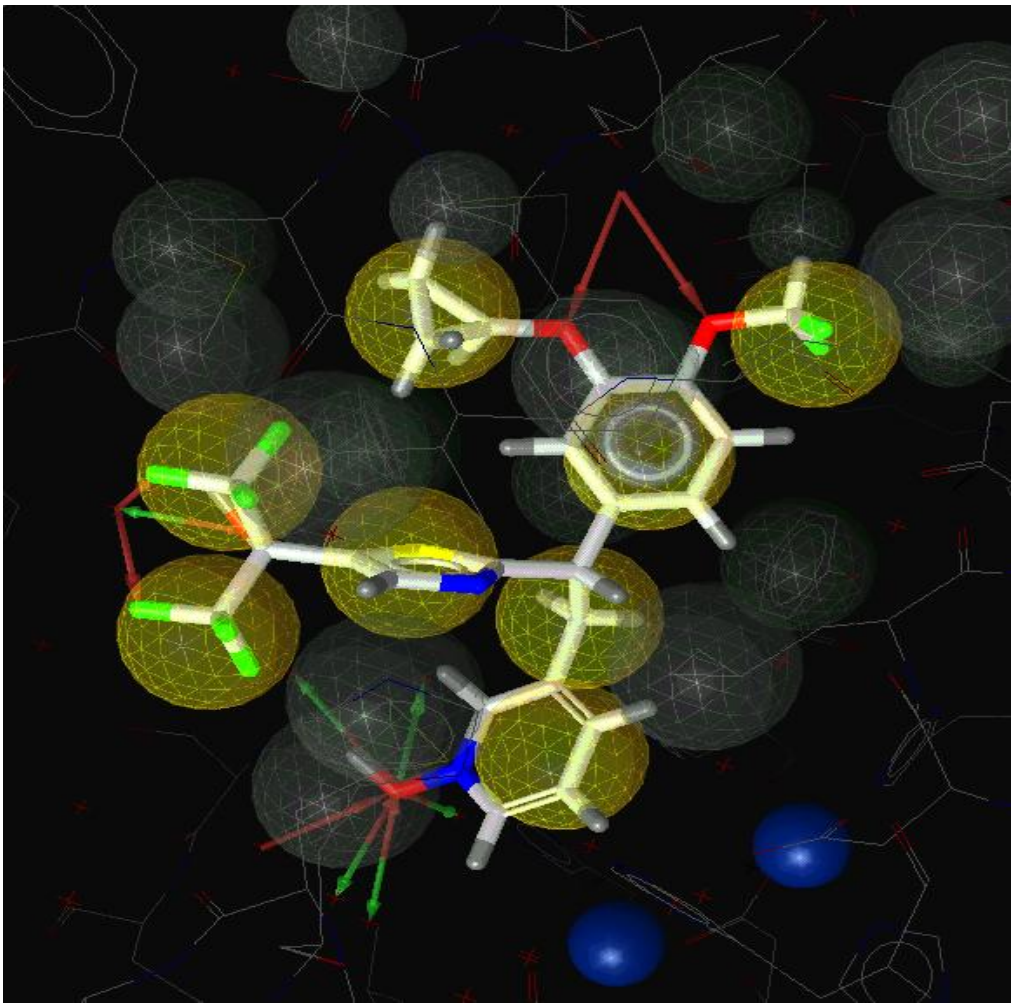

Figure 4.4. 2FM0 pharmacophore model prepared with LigandScout

In the the fourth and last model (Figure 4.4), the natural ligand is L-269298. This model is a little bit different  than the other 3 models. The same part is that there is an aromatic ring and at the top of the molecule the oxygens interact with the GLN 443A residue. On the other hand, there is another big functional group in the left side and maybe this can bind through the active site better and will be a good scaffold to find new candidate compounds for PDE4 inhibitors.

After preparing the pharmacophores with LigandScout, these models were refined with another software: Catalyst. But before the refinement, screening was performed for several databases according to these 4 pharmacophore models and the 1st model, 1RO6 model (Figure 5.1), gave compounds which resemble to natural ligand of 1RO6 enzyme and also gave different compounds which can be a new scaffold for design of PDE4 inhibitors. So it was decided to focus on 1RO6 pharmacophore model and started to refine it with adding excluded volumes. And also the shape of 2FM0 was considered and was put in 1RO6 pharmacophore in order to find more specific compounds which have the structure shape of 2FM0's ligand.

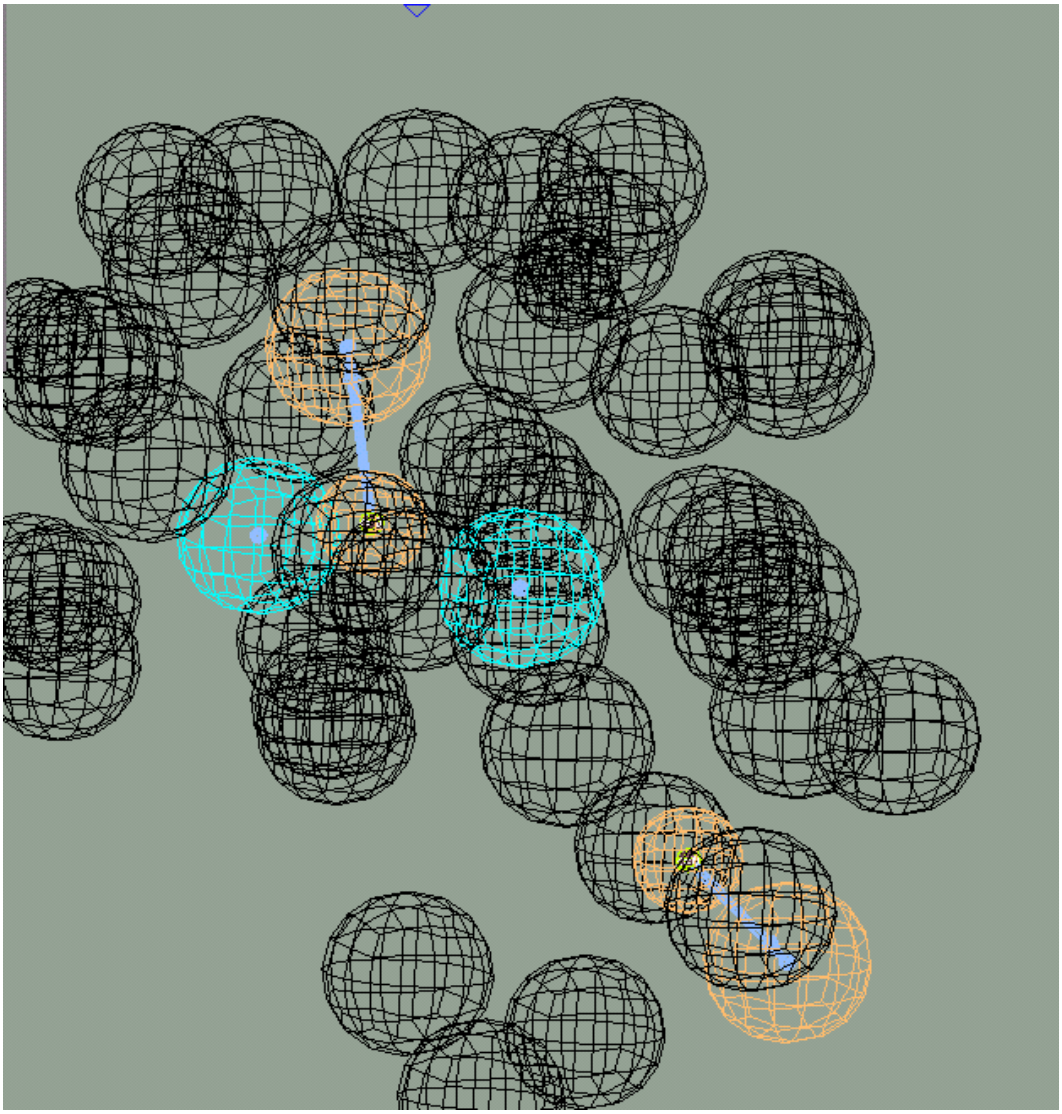

Figure 4.5. 1RO6 model with Catalyst program

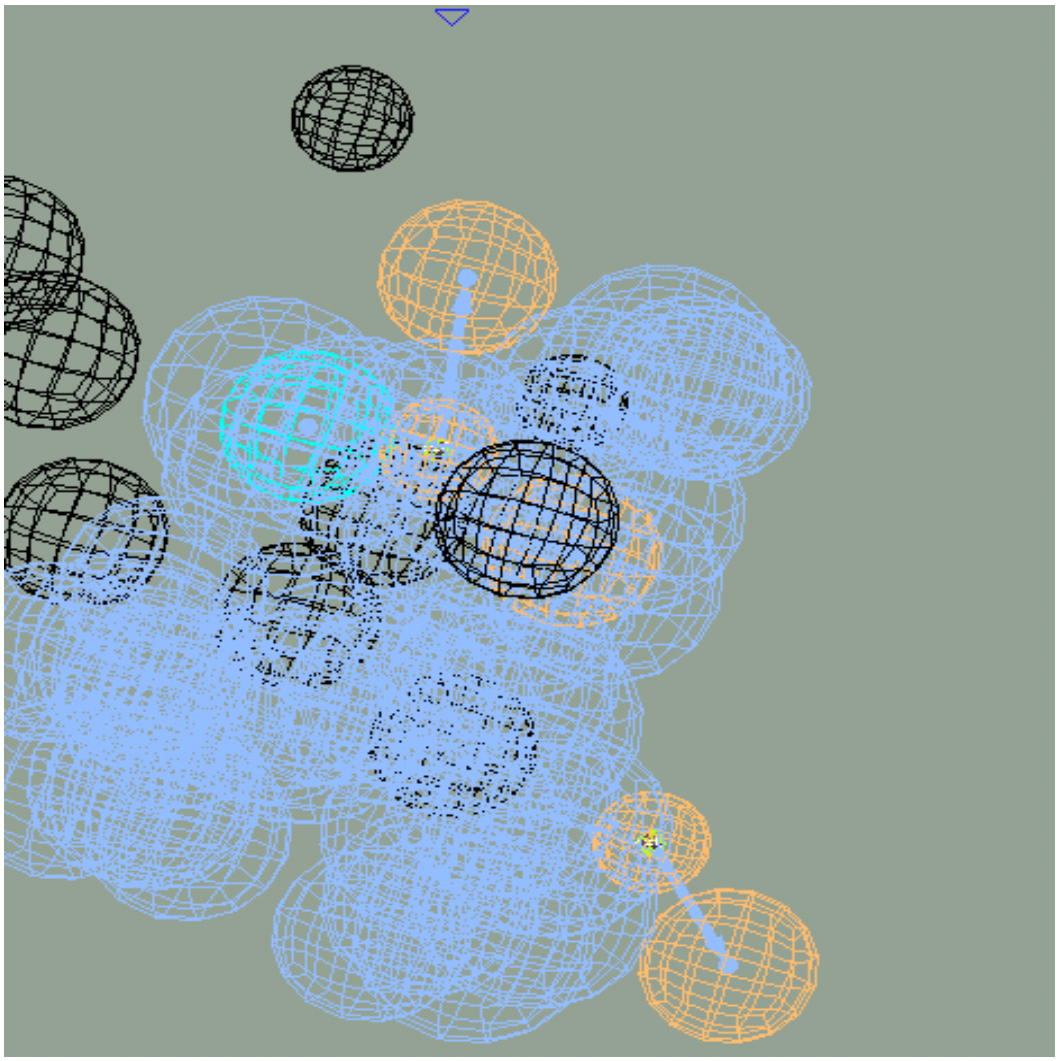

Figure 4.6. 1RO6 simpleshape-2FM0 pharmacophore model

In 1RO6 simpleshape-2FM0 pharmacophore model, the blue spherical shape represent the structure of the natural ligand of 2FM0 X-ray crytal structure. This shape was put on the 1RO6 ligand shape in order to develop a scaffold for PDE4 inhibitors.

Then the ligands from the pharmacophore models were aligned with the MOE software (Figure 4.7. ).

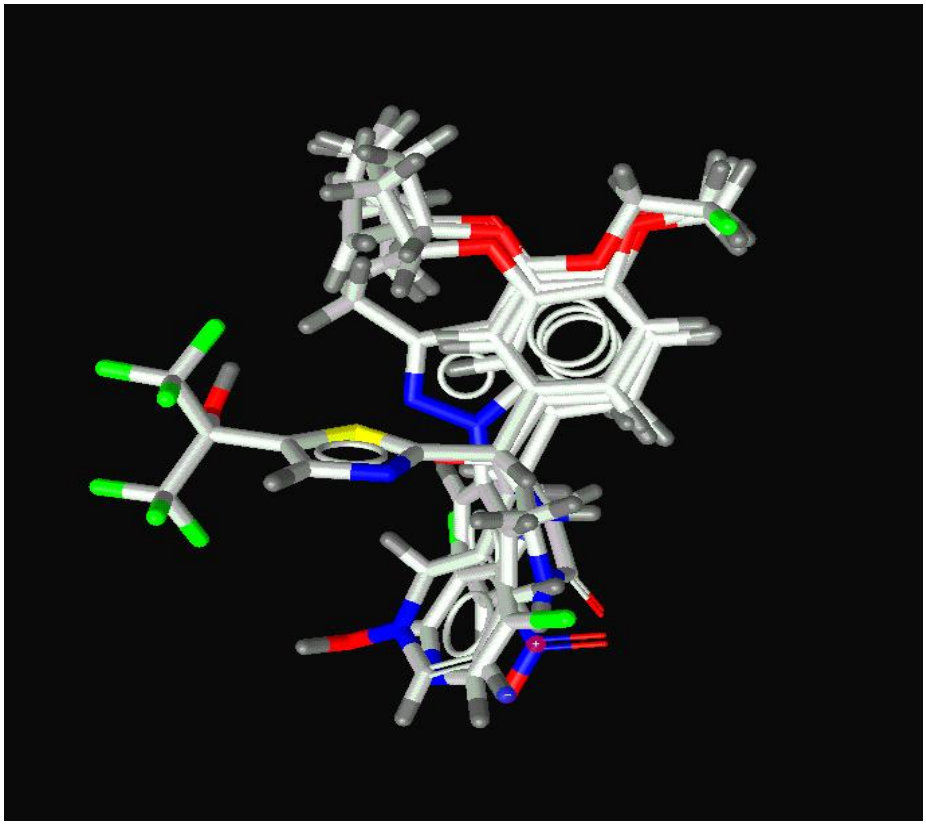

Figure 4.7. Ligand alignment with MOE software

As seen in Figure 4.7., the ligand alignment is very well and only the part which goes to the left side is different because it comes from only 2FM0 model .

After finishing the pharmacophore models refinement, virtual screening with several databases according to the final refined 1RO6 pharmacophore model was carried out. The databases are:

- Chembridge Library
- Maybridge Library
- Asinex-Gold Library
- Asinex-Platinum Library
- Specs database

- NCI (National Cancer Institute)

In these libraries, there have been about 2 million drug-like compounds and at the end of virtual screening according to 1RO6 pharmacophore model, 1959 hit compounds were obtained for further steps in this study.

### 4.2. Docking with AutoDock 4.0 program

After screening several databases, to filter the compounds, docking process was performed in this part of the study but before the docking process Lipinski's rule of fives was applied such as:

i. The molecular weight is lower than 500,
ii. The log*P* is smaller than five,
iii. There are less than five hydrogen bond donors (defined as the sum of OH and NH groups),
iv. There are less than ten hydrogen bond acceptors (defined as the number of N and O atoms),
v. There are less than eight rotatable bonds.

MOE program was used to calculate these 4 rules and eliminate the compounds which didn't satisfy the rules so there were 1840 compounds for docking process.

AutoDock 4.0 software program was used for docking process. In the docking process, the macromolecule was 1RO6 enzyme because we focused on the pharmacophore model belonging to this enzyme. The aminoacid A chain, 2 divalent metal ions $Zn^{+2}$ and $Mg^{+2}$, and also 1 water molecule ($H_2O$ 788A residue) were considered because this can give important interactions in the active site of the enzyme as shown in the pharmacophore models before (Figure 4.1, 2, 3, and 4.).

The natural ligand rolipram was docked into the 1RO6 active site because this is the reference molecule. 10 runs for rolipram were performed (see Appendix B).

Table 4.1. Docking results for ligand rolipram with AutoDock 4.0

| **Rank** | **Sub-Rank** | **Run** | **Binding Energy(kcal/mol)** | **Reference RMSD** |
|---|---|---|---|---|
| **1** | **1** | **2** | **-8.17** | **0.81** |
| **1** | **2** | **5** | **-8.16** | **0.79** |
| **1** | **3** | **10** | **-8.16** | **0.79** |
| **1** | **4** | **1** | **-8.16** | **0.78** |
| **1** | **5** | **9** | **-8.16** | **0.82** |
| **1** | **6** | **8** | **-8.16** | **0.80** |
| **1** | **7** | **4** | **-8.16** | **0.78** |
| **1** | **8** | **3** | **-8.00** | **0.86** |
| **1** | **9** | **6** | **-7.27** | **1.53** |
| **2** | **1** | **7** | **-6.13** | **18.85** |

As seen in Table 4.1. , after the docking process with AutoDock 4.0, the binding energies and RMSD values for each run were obtained. The results are classified in ranks and also each run is divided into sub-ranks. For the natural ligand rolipram, the run number 2 which belongs to rank 1 and also sub-rank 1, is the best pose based on binding energies (-8.17 kcal/mol) and it has 0.81 RMSD value.

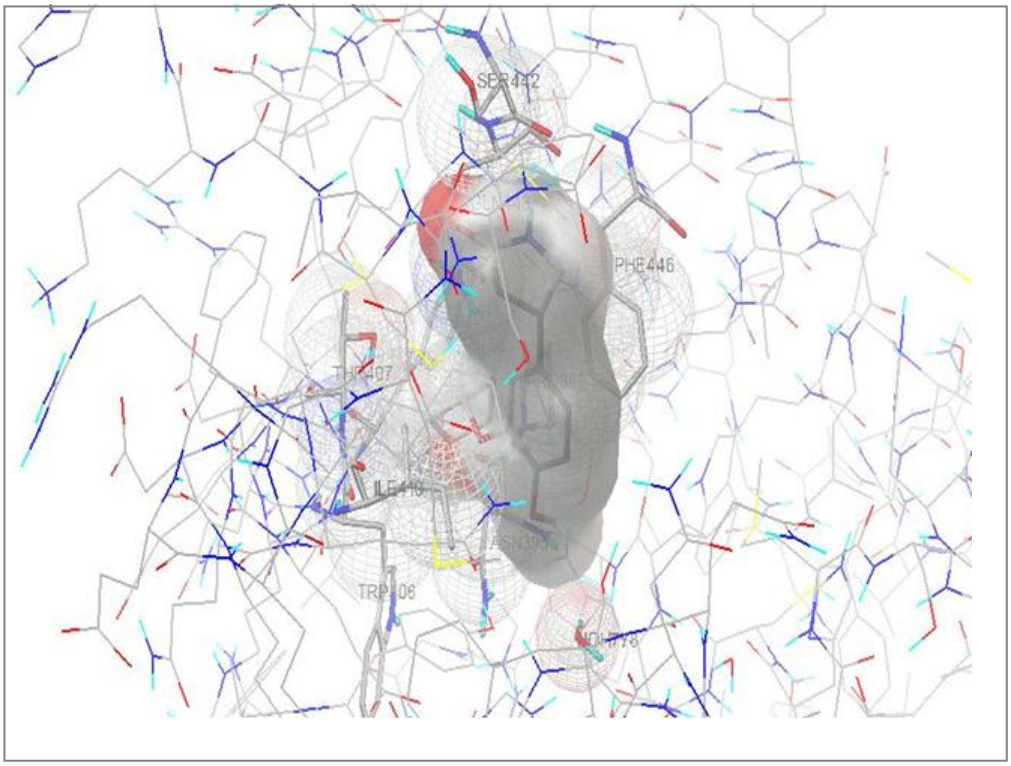


Figure 4.8. Best pose of rolipram docked into the active site of 1RO6 with AutoDock 4.0.

After the natural ligand rolipram, all of the hit compounds were prepared for docking and high-throughput screening with AutoDock 4.0 was done (see Appendix B). Again for each ligand, 10 runs were carried out for docking.

Also with the AutoDock 4.0 program, $K_i$ (dissociation constant) was obtained for each run during the docking process.

$K_i$ is the dissociation constant and it is a measure how tightly a ligand binds to a protein. So if $K_i$ is low, the ligand shows high affinity; if $K_i$ is high, the ligand has low affinity to bind the target protein. It is desirable to have low $K_i$ values to have high affinity to bind the macromolecule.

We had 1840 candidate molecules before docking and we used the docking process for filtering the compounds. For each ligand, the binding energies were checked and the compounds which have binding energies better than rolipram were chosen. 100 molecules have been obtained, which have a better energy than natural ligand rolipram.

Also with a C program (rmsd_$K_i$_min.c), the information of RMSD values and the dissociation constant values for the selected compounds (see Appendix B).

Table 4.2. Energy values for the top 100 molecules after docking AutoDock 4.0.

| **sample_id** | **run_id** | **rmsd** | **energy (kcal/mol)** |
|---|---|---|---|
| rolipram | 2.00 | 0.810 | -8.17 |
| 1586.0 | 3.00 | 3.830 | -14.450 |
| 1323.0 | 6.00 | 2.890 | -14.200 |
| 1017.0 | 7.00 | 3.990 | -13.340 |
| 1890.0 | 6.00 | 2.750 | -12.990 |
| 1831.0 | 1.00 | 2.880 | -12.910 |
| 1463.0 | 5.00 | 3.820 | -12.880 |
| 392.0 | 3.00 | 2.810 | -12.540 |
| 532.0 | 8.00 | 2.930 | -12.490 |
| 1741.0 | 9.00 | 3.920 | -12.370 |
| 319.0 | 5.00 | 2.050 | -12.310 |
| 962.0 | 9.00 | 3.270 | -12.290 |
| 545.0 | 6.00 | 2.020 | -12.240 |
| 497.0 | 2.00 | 3.430 | -12.220 |
| 438.0 | 4.00 | 2.180 | -12.060 |
| 999.0 | 3.00 | 2.330 | -11.900 |
| 976.0 | 5.00 | 2.320 | -11.850 |
| 1465.0 | 1.00 | 2.150 | -11.780 |
| 1363.0 | 4.00 | 3.260 | -11.760 |
| 105.0 | 6.00 | 2.920 | -11.560 |
| 1287.0 | 6.00 | 8.190 | -11.540 |
| 761.0 | 6.00 | 3.440 | -11.450 |
| 472.0 | 3.00 | 4.720 | -11.440 |
| 1404.0 | 4.00 | 4.070 | -11.440 |
| 1334.0 | 7.00 | 1.530 | -11.410 |
| 76.0 | 3.00 | 4.780 | -11.400 |
| 933.0 | 4.00 | 3.810 | -11.380 |
| 334.0 | 3.00 | 3.770 | -11.320 |
| 1324.0 | 1.00 | 5.760 | -11.320 |
| 1736.0 | 6.00 | 5.730 | -11.320 |
| 380.0 | 3.00 | 4.550 | -11.310 |
| 1780.0 | 6.00 | 3.460 | -11.280 |
| 869.0 | 3.00 | 1.900 | -11.230 |

Table 4.2.continued.

| | | | |
|---|---|---|---|
| 1453.0 | 7.00 | 2.550 | -11.210 |
| 972.0 | 7.00 | 3.510 | -11.200 |
| 1318.0 | 5.00 | 5.150 | -11.170 |
| 1531.0 | 8.00 | 6.470 | -11.170 |
| 1738.0 | 4.00 | 6.520 | -11.170 |
| 928.0 | 9.00 | 2.750 | -11.160 |
| 957.0 | 10.00 | 6.100 | -11.140 |
| 1785.0 | 5.00 | 5.950 | -11.130 |
| 1808.0 | 8.00 | 3.270 | -11.120 |
| 1446.0 | 7.00 | 2.360 | -11.090 |
| 16.0 | 1.00 | 2.210 | -11.060 |
| 84.0 | 1.00 | 5.160 | -11.050 |
| 868.0 | 2.00 | 3.930 | -11.050 |
| 1613.0 | 2.00 | 6.550 | -11.050 |
| 1420.0 | 9.00 | 2.510 | -11.030 |
| 862.0 | 5.00 | 1.310 | -11.020 |
| 348.0 | 4.00 | 7.070 | -10.990 |
| 1028.0 | 9.00 | 3.920 | -10.970 |
| 1451.0 | 6.00 | 1.940 | -10.970 |
| 1749.0 | 3.00 | 5.650 | -10.970 |
| 788.0 | 3.00 | 3.850 | -10.960 |
| 1152.0 | 6.00 | 7.030 | -10.950 |
| 388.0 | 7.00 | 3.630 | -10.930 |
| 918.0 | 1.00 | 3.550 | -10.930 |
| 1619.0 | 5.00 | 5.240 | -10.930 |
| 766.0 | 7.00 | 2.620 | -10.900 |
| 1694.0 | 8.00 | 5.810 | -10.890 |
| 1767.0 | 4.00 | 1.830 | -10.890 |
| 397.0 | 8.00 | 3.630 | -10.880 |
| 1089.0 | 9.00 | 2.110 | -10.880 |
| 1073.0 | 6.00 | 2.080 | -10.880 |
| 657.0 | 4.00 | 2.070 | -10.870 |
| 1200.0 | 4.00 | 3.630 | -10.870 |
| 485.0 | 2.00 | 5.060 | -10.860 |
| 1202.0 | 2.00 | 1.700 | -10.850 |
| 1501.0 | 2.00 | 3.730 | -10.850 |
| 1483.0 | 9.00 | 2.350 | -10.840 |
| 201.0 | 3.00 | 2.260 | -10.830 |
| 1727.0 | 1.00 | 2.480 | -10.830 |
| 1294.0 | 3.00 | 3.750 | -10.820 |
| 1241.0 | 10.00 | 1.780 | -10.820 |

Table.4.2.continued.

| | | | |
|---|---|---|---|
| 1686.0 | 2.00 | 3.340 | -10.820 |
| 637.0 | 5.00 | 7.070 | -10.810 |
| 1410.0 | 5.00 | 3.280 | -10.810 |
| 1799.0 | 6.00 | 6.880 | -10.800 |
| 1072.0 | 2.00 | 3.550 | -10.790 |
| 267.0 | 9.00 | 6.470 | -10.770 |
| 817.0 | 6.00 | 8.200 | -10.690 |
| 689.0 | 5.00 | 5.090 | -10.680 |
| 1684.0 | 10.00 | 2.880 | -10.680 |
| 1542.0 | 6.00 | 2.240 | -10.670 |
| 786.0 | 5.00 | 7.350 | -10.620 |
| 1261.0 | 8.00 | 6.090 | -10.600 |
| 577.0 | 4.00 | 3.380 | -10.580 |
| 961.0 | 4.00 | 5.570 | -10.580 |
| 476.0 | 10.00 | 3.210 | -10.560 |
| 1282.0 | 6.00 | 3.380 | -10.560 |
| 1262.0 | 6.00 | 2.930 | -10.560 |
| 510.0 | 3.00 | 3.410 | -10.550 |
| 96.0 | 9.00 | 1.960 | -10.520 |
| 1148.0 | 8.00 | 4.640 | -10.520 |
| 479.0 | 3.00 | 3.060 | -10.500 |
| 672.0 | 3.00 | 2.520 | -10.500 |
| 1792.0 | 10.00 | 3.020 | -10.500 |
| 1414.0 | 8.00 | 2.210 | -10.490 |
| 1795.0 | 10.00 | 3.020 | -10.490 |
| 1000.0 | 4.00 | 2.680 | -10.480 |
| 765.0 | 4.00 | 2.480 | -10.460 |

The strain energy as the difference between the best pose of the ligands after the docking process with AutoDock 4.0 [81] and the optimized conformation of ligands with Spartan 04 was calculated. Also the strain energy (ΔE) was calculated with MOE and Spartan.

Table 4.3. Strain energies (ΔE, kcal/mol) calculated with MMFF94x and PM3.

| Sample_id. | ΔE (PM3) | ΔE (MMFF94x) | $K_i$ values from AutoDock4 |
|---|---|---|---|
| rolipram | 17.65 | 24.07 | 1.03 μM |
| 689.0 | 23.61 | 16.13 | 14.89 nM |
| 319.0 | 29.64 | 63.41 | 940.78 pM |
| 637.0 | 30.09 | 47.63 | 11.98 nM |
| 16.0 | 31.64 | 45.96 | 7.78 nM |
| 532.0 | 33.82 | 25.67 | 697.08 pM |
| 105.0 | 34.29 | 23.49 | 3.34 nM |
| 388.0 | 36.35 | 8.54 | 9.66 nM |
| 267.0 | 46.54 | 51.16 | 12.82 nM |
| 380.0 | 47.04 | 50.60 | 5.13 nM |
| 348.0 | 47.18 | 54.57 | 8.80 nM |
| 76.0 | 51.67 | 143.93 | 4.42 nM |
| 397.0 | 53.23 | 70.33 | 10.63 nM |
| 485.0 | 121.53 | 95.16 | 11.01 nM |
| 472.0 | 194.34 | 125.04 | 4.11 nM |
| 497.0 | 331.97 | 91.51 | 1.10 nM |
| 545.0 | 765.23 | 503.52 | 1.07 nM |

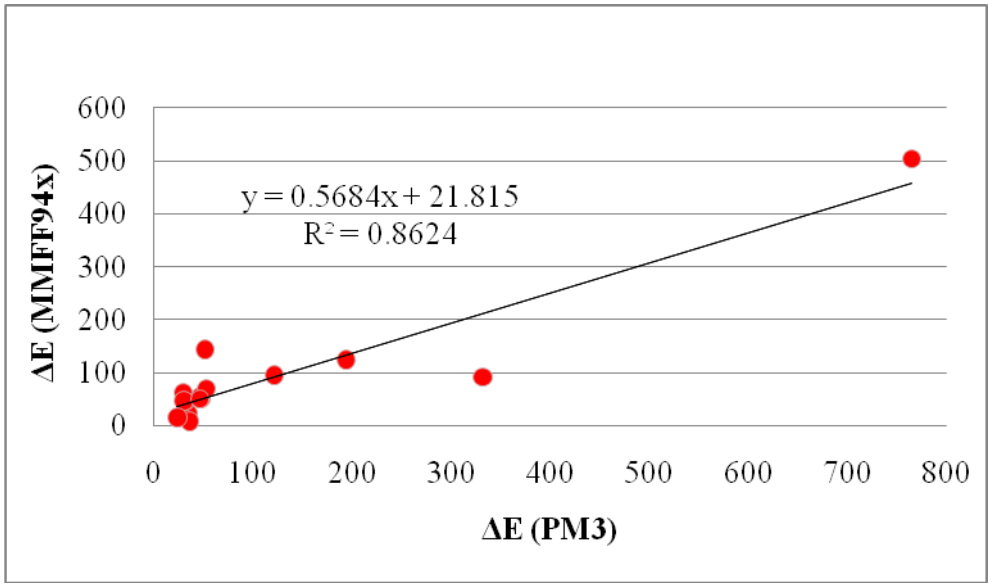


Figure 4.9. ΔE in PM3 vs. ΔE in MMFF94x (kcal/mol).

From Table 4.3., it can be seen that the natural ligand rolipram has a strain energy lower than 20 kcal/mol and some of the selected candidate molecules have strain energy values close to rolipram. Also, there is a good correlation between strain energies calculated with PM3 and MMFF94x (Figure 4.9).

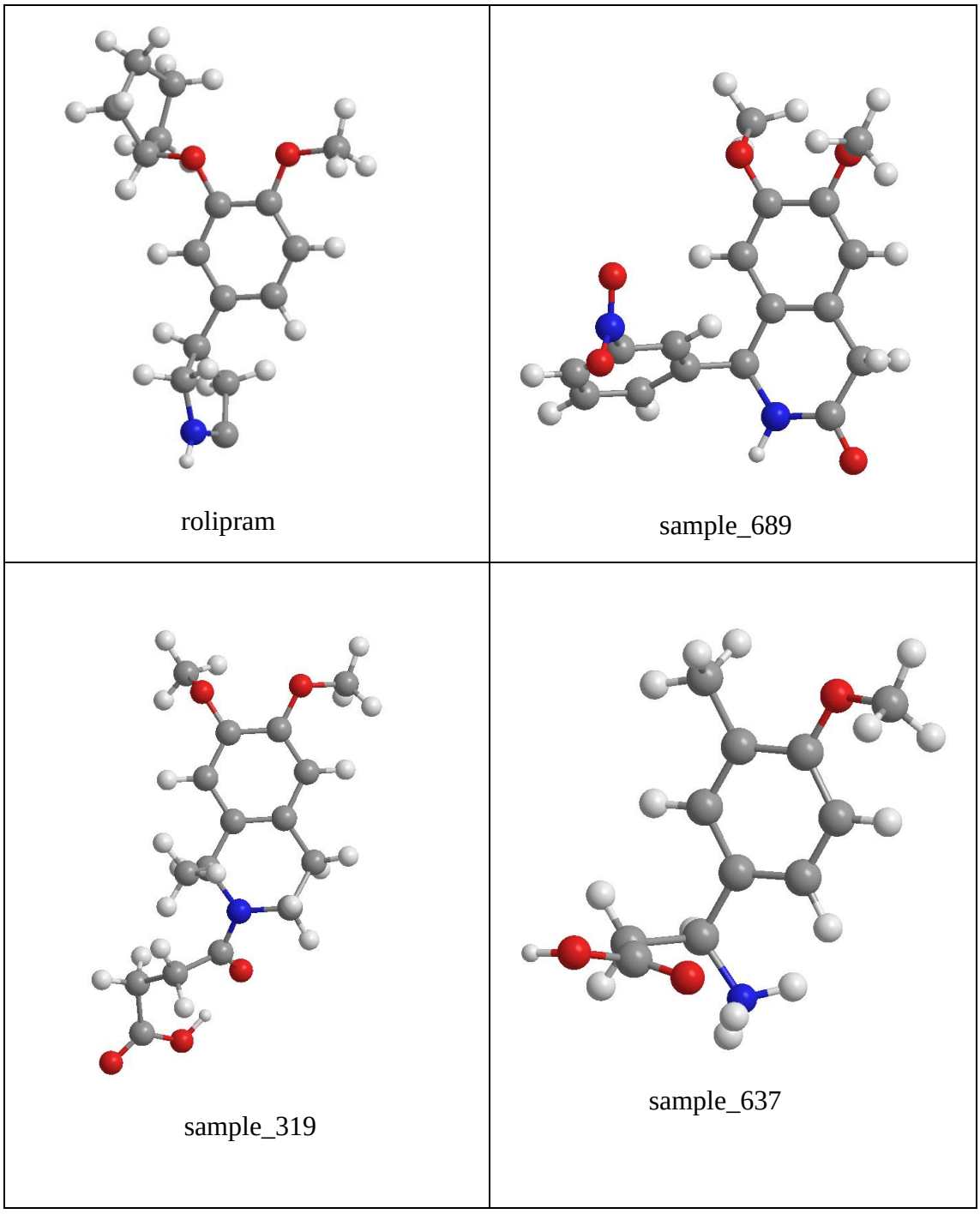


Figure 4.10. Structures of candidate molecules drawn with Chem-3D Ultra.

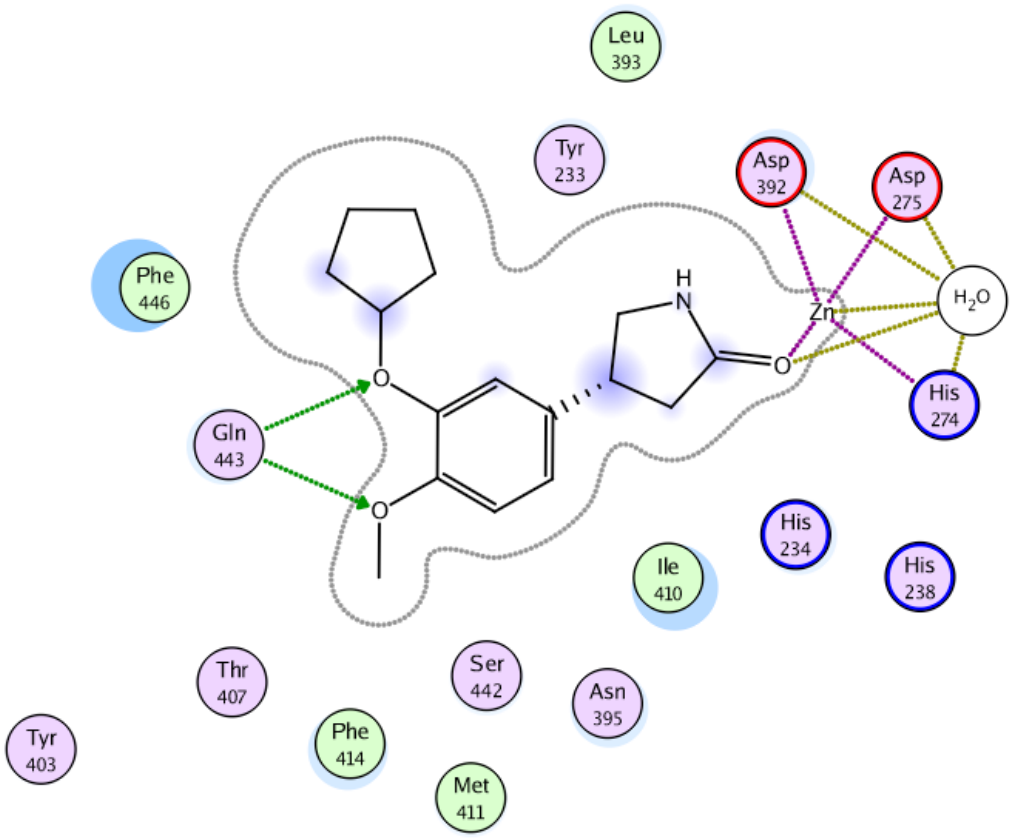


Figure 4.11. Ligand interactions of rolipram (MOE).

As shown in Figure 4.11., there are important interactions with residues and metal ion $Zn^{+2}$ in the active site of 1R06. The metal ion $Zn^{+2}$ is coordinated with 5 molecules, 3 of them (Asp 392, Asp 375, His 274) are amino acid residues, one of them is water molecule ($H_2O$ 788 A) and last one is the carbonyl oxygen bonded to five-membered ring on the ligand rolipram. Also the water molecule ($H_2O$ 788 A) is interacting with the same carbonyl oxygen on the rolipram. Another important interaction is between Gln 443 A residue and the oxygen atoms bonded to the aromatic ring. The residues around the active site, that can have important roles in binding, are Phe 446, Thr 407, Tyr 403, Phe 414, Met 411, Ser 442, Asn 395, Ile 410, His 234, His 238, Tyr 233 and Leu 393.

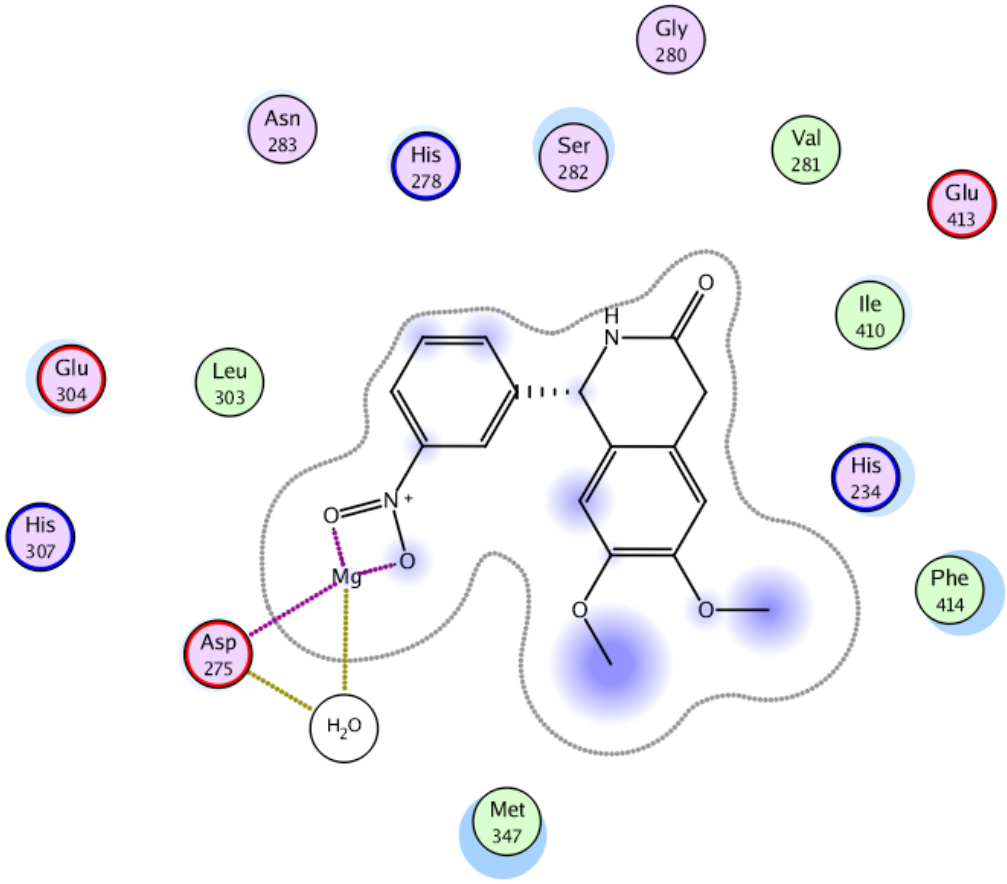


Figure 4.12. Ligand interactions of sample_689 (MOE).

In Figure 4.12., residues around 6.5 Å proximity within the active site of 1RO6 are shown. The important residues are His 307, Glu 304, Leu 303, Asn 238, His 278, Ser 282, Val 281, Glu 413, Ile 410, His 234, Phe 414, Met 347, Asp 275 and the water molecule ($H_2O$ 788 A). The $Mg^{+2}$ ion is coordinated with Asp 275 residue, water molecule ($H_2O$ 788 A) and the oxygen atoms which are bonded to $N^{+}$.

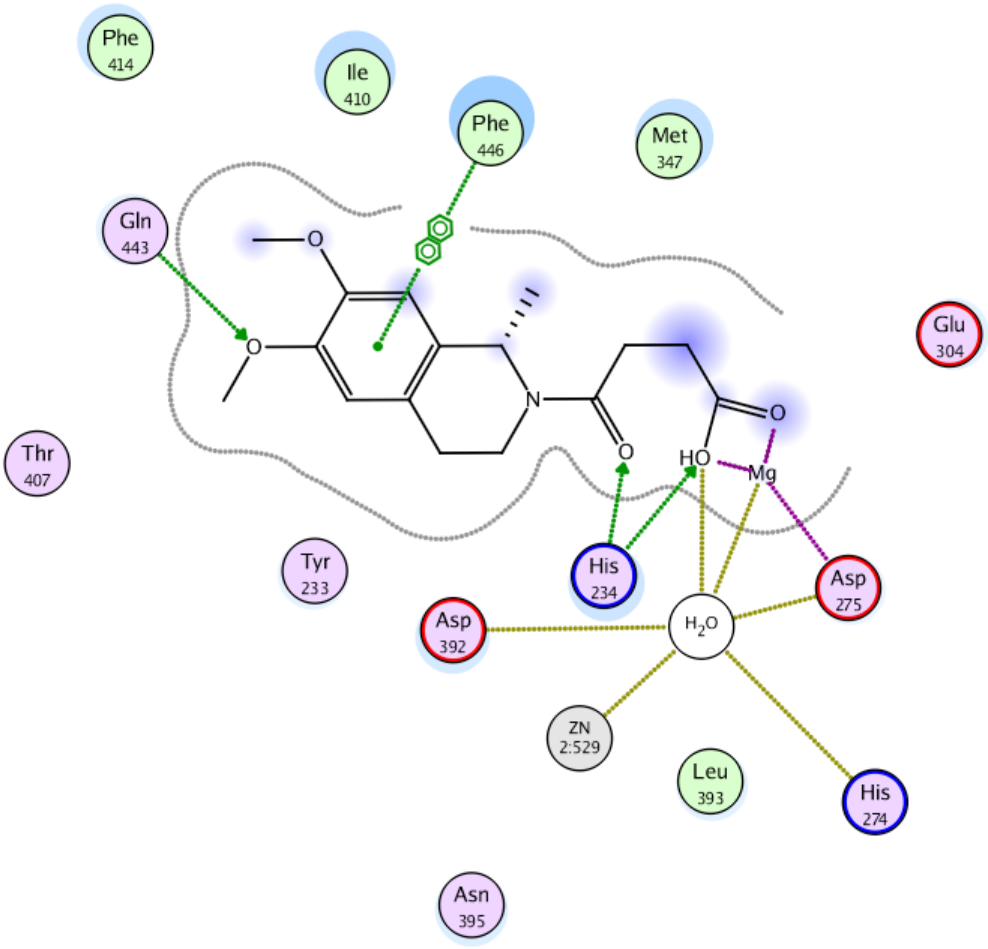


Figure 4.13. Ligand interactions of sample_319 (MOE).

$Mg^{+2}$ ion is coordinated with Asp 275 residue, water molecule ($H_2O$ 788 A) and the oxygen atoms (-OH and =O) on the ligand 319. Also the water molecule gives interaction with His 274, Asp 275 and Asp 392 aminoacid residues, $Zn^{+2}$ and $Mg^{+2}$ ions and oxygen atom on the ligand (-OH). Another important interaction is between His 234 residue and the oxygen atoms on the ligand (-OH and =O). Gln 443 interacts with oxygen atom bonded to the aromatic ring same as rolipram (Figure 5.11.). Other important residues are Phe 414, Ile 410, Phe 446, Met 347, Glu 304, Asn 395, Tyr 233, and Thr 407.

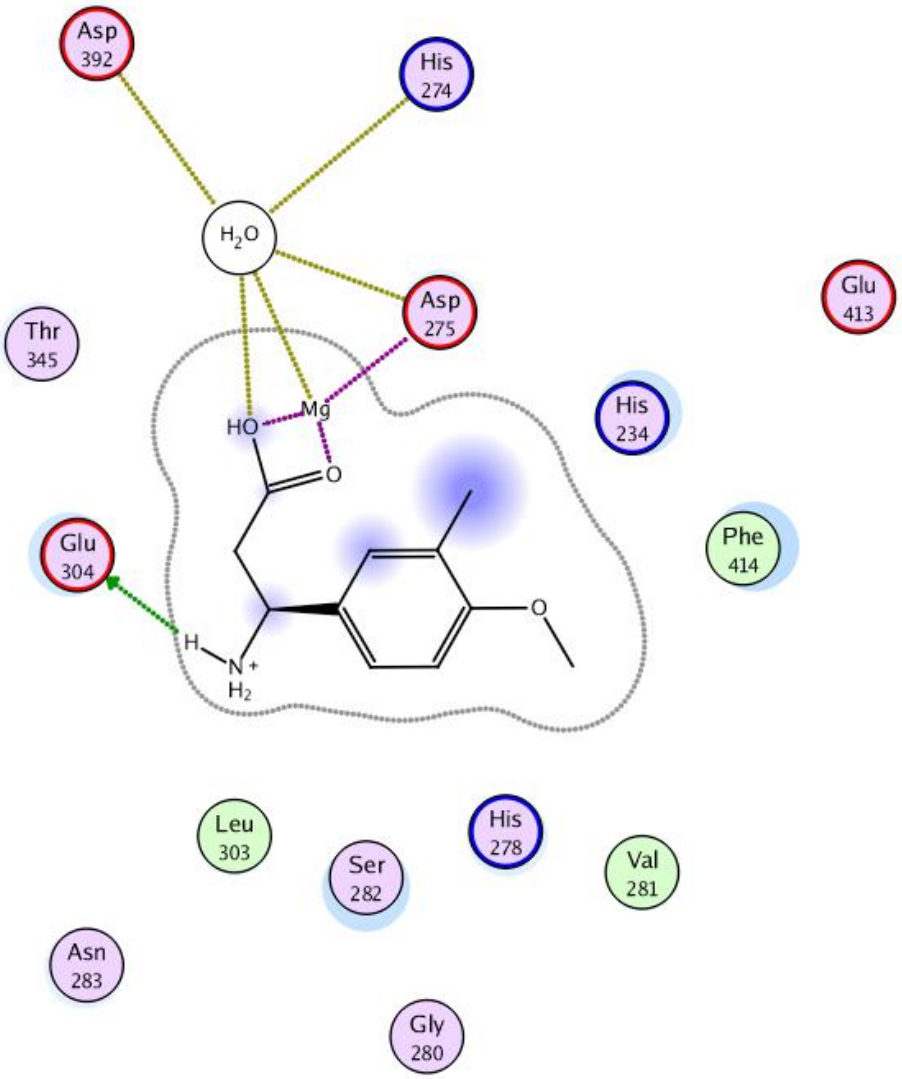


Figure 4.14. Ligand interactions of sample_637 (MOE).

Thr 345, Glu 304, Asn 283, Leu 303, Ser 282, His 278, Gly 280, Val 281, Phe 414, His 234, Glu 413, Asp 275, His 274 and Asp 392 are important residues for binding of ligand 637. Among these residues, Asp 392, His 274 and Asp 275 interact with water molecule ($H_2O$ 788 A) and also Asp 275, water molecule and oxygen atoms (-OH and =O) on the ligand coordinates $Mg^{+2}$ ion. And there is another interaction between Glu 304 and H atom attached to the $NH_2$.

When comparing these candidate molecules with the natural ligand rolipram, it is seen that Phe 414, His 234 and Asp 275 residues are common residues among them. Also it is understood that the water molecule ($H_2O$ 788 A) should be kept during the docking process because it is close to some residues and give interactions with them and also with metal ions $Mg^{+2}$ and $Zn^{+2}$ (Figure 4.11.- 14. ).The metal ions $Zn^{+2}$ and $Mg^{+2}$ are coordinated with aminoacid residues around the active site, with water molecule and some atoms on the ligand molecule (Figure 4.11.- 14.).

# 5. CONCLUSION AND FUTURE WORK

In this study a scaffold-based drug discovery paradigm has been applied to PDE4. This begins with the modeling of pharmacophores for PDE4 natural inhibitor rolipram and then virtual screening of drug-like compound libraries to identify similar novel compounds. This is followed by docking process of natural ligand rolipram and other molecules. At the end, strain energies are calculated for candidate molecules.

In the candidate molecules, the oxygen atoms that are bonded to aromatic ring interacts with Gln 443A residue so in order to maintain this interaction the oxygen atoms should be fixed and different functional groups can be attached to these atoms. At the same time, the electronegative elements like nitrogen, oxygen and fluorine interact with $H_2O$ 788A residue and also these elements may have interaction with the $Zn^{+2}$ metal ion, these interactions may be considered for designing new compounds.

For future work;

- ADME (absorption, distribution, metabolism, and excretion), toxicity, and solubility properties can be calculated and analyzed for candidate compounds.
- The study will be repeated with other pharmacophores.
- The screening will be carried out based on binding energies and ADME (absorption, distribution, metabolism, excretion) properties.
- The ligand-substrate binding energies will be calculated with semi-empirical methods.
- It is also desirable to perform MD simulations on several substrate-enzyme complexes and confirm the semi-empirical binding energies.

# APPENDIX A

## A.1. AutoDock 4 is Free Software

The introduction of AutoDock 4 comprises three major improvements:

- The docking results are more accurate and reliable.
- It can optionally model flexibility in the target macromolecule.
- It enables AutoDock's use in evaluating protein-protein interactions.

AutoDock 4 is free and is available under the GNU General Public License. Autodock 4.0 is currently in beta testing. It allows side chains in the macromolecule to be flexible, as well as allowing for ligand flexibility. Autodock 4.0 adds a free-energy scoring function created from a linear regression analysis, the AMBER force field, and a large set of diverse protein-ligand complexes with known inhibiton constants. Previous versions of Autodock used a scoring function that computed a binding energy based on the AMBER force field, but was reparametrized specifically for docking. The searching algorithms include simulated annealing and a genetic algorithm.

## A.2. Why Use Grid Maps?

- Saves time:
  i. Pre-computing the interactions on a grid is typically 100 times faster than traditional Molecular Mechanics methods,
  ii. $O(N^2)$ calculation becomes O(N).
- AutoDock uses trilinear interpolation to compute the score of a candidate docked ligand conformation,
- AutoDock needs one map for each atom type in the ligand(s) and moving parts of receptor (if there are any).
- Drawback: The receptor is conformationally rigid (although ‘vdW softened’),
- Limits the search space.

## A.3. Setting up the AutoGrid Box

- The macromolecule atoms will be in the rigid part
- The center contains:
  i. center of ligand;
  ii. center of macromolecule;
  iii. a picked atom; or
  iv. typed-in x-, y- and z-coordinates.
- Grid point spacing:
- The default value  is 0.375Å (from 0.2Å to 1.0Å: ).
- Number of grid points in each dimension:
  i. only give even numbers (from 2 × 2 × 2 to 126 × 126 × 126).
  ii. AutoGrid adds one point to each dimension.
- Grid Maps depend on the orientation of the macromolecule.
- Make sure all the flexible parts of the macromolecule are inside the grid.

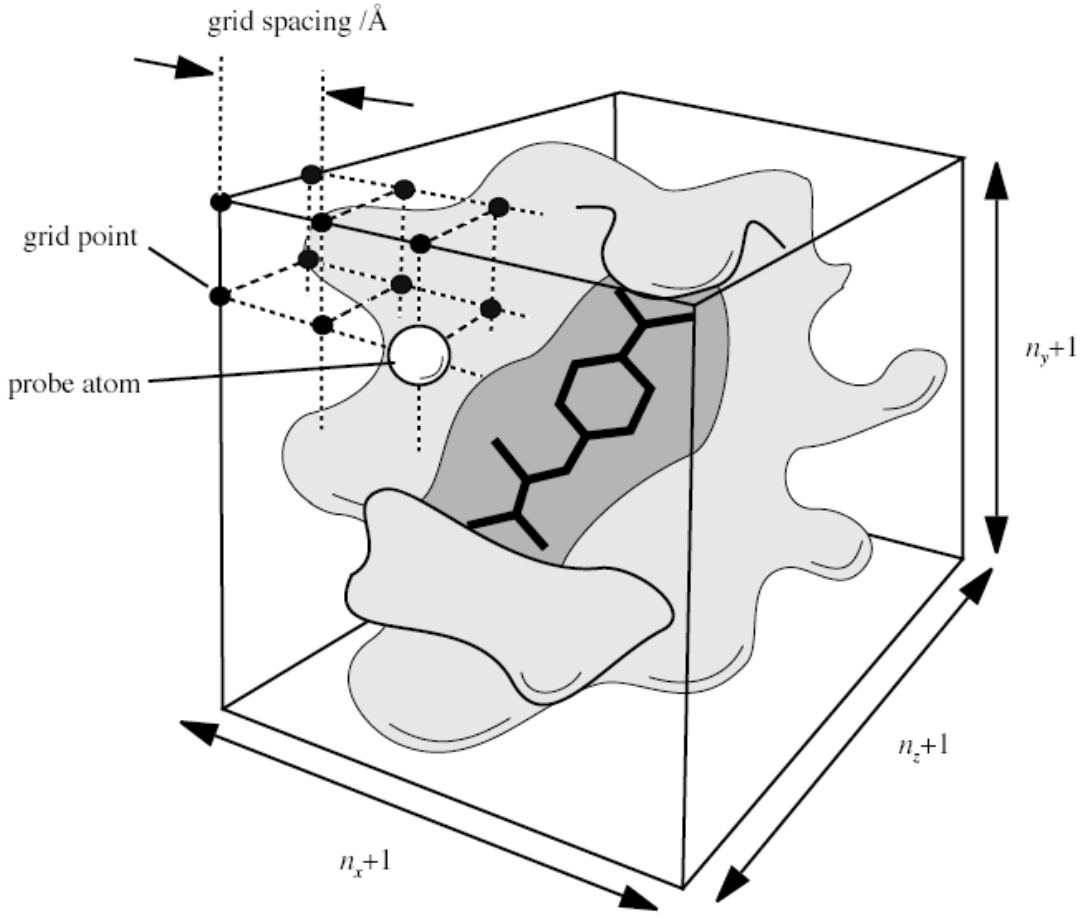


Figure A.1. Grid box picture in AutoDock.

### A.4. Using AutoDock Step-by-Step

- Set up ligand PDBQT: using ADT's "Ligand" menu
- OPTIONAL: Set up flexible receptor PDBQT: using ADT's "Flexible Residues" menu
- Set up macromolecule & grid maps: using ADT's "Grid" menu
- Pre-compute AutoGrid maps for all atom types in your set of ligands: using "autogrid4"
- Perform dockings of ligand to target: using "autodock4", and in parallel if possible.
- Visualize AutoDock results: using ADT's "Analyze" menu

- Cluster dockings: using “analysis” DPF command in “autodock4” or ADT’s “Analyze” menu for parallel docking

### A.5. AutoDock 4 File Formats

- Prepare the following Input Files:
    i. Ligand PDBQT file
    ii. Rigid Macromolecule PDBQT file
    iii. Flexible Macromolecule PDBQT file (“Flexres”)
    iv. AutoGrid Parameter File (GPF)
    v. GPF depends on atom types in:
    vi. Ligand PDBQT file
    vii. Optional flexible residue PDBQT files)
    viii. AutoDock Parameter File (DPF)
- Run AutoGrid 4:

Macromolecule PDBQT + GPF → Grid Maps, GLG

- Run AutoDock 4:

Grid Maps + Ligand PDBQT + [Flexres PDBQT +] DPF → DLG (dockings and clustering)

- Run ADT to Analyze DLG

### A.6. Preparing Ligands and Receptors with AutoDock 4

- Ligand:
    i. Add all hydrogens, compute Gasteiger charges, and merge non-polar H; also assign AutoDock 4 atom types
    ii. Ensure total charge corresponds to tautomeric state
    iii. Choose torsion tree root and rotatable bonds

- Macromolecule:
    i. Add all hydrogens, compute Gasteiger charges, and merge non-polar H; also assign AutoDock 4 atom types
    ii. Assign Stouten atomic solvation parameters

- Optionally, create a flexible residues PDBQT in addition to the rigid PDBQT file
- Compute AutoGrid maps
- AutoDock uses ‘United Atom’ model so it reduces number of atoms and speeds up
- docking
- Add polar Hs. and remove non-polar Hs.
- Consider pH for acidic and basic residues,
- Histidines.(http://molprobity.biochem.duke.edu/)
- Other molecules in receptor: waters, cofactors, and  metal ions.

# APPENDIX B

## B.1. Creating Files with AutoDockTools

The following actions have been performed in a row like that:

- Download pdb file of 1RO6 enzyme from the Protein Databank.
- Delete B aminoacid chain, the ligands in the both A and B chains, the metal ions belongs to this chain and also the water molecules but when deleting the water molecules, looked the active site and selected 6.5 $A^0$ proximity within the ligand rolipram. The $H_2O$ 788A residue is so close to the ligand and gives essential interaction in the active site so this water molecule was kept during the docking process.
- Protonate the enzyme in the MOE program and save as *.pdb format.
- Open the molecule in the AutoDockTools (ADT) interface.
- Read→Molecule→Edit→Hydrogens→Merge Nonpolar Hydrogens→Save as PDB.
- Grid→Macromolecules→Open PDB→Save PDBQT.
- Open the file with "vi" and add the metal ions and their x,y,z coordinate values into the file because in the ADT, the file as PDBQT format can not be saved with metal ions. Also, add the charges as +2 for Zn and Mg ions.
- Calculate the overall charge (Gasteiger Charge) in the ADT and it gave a non-integer value so change the Zn and Mg charges from +2 to +1.96 and at the end obtain an integer charge value for whole the molecule.
- Before saving the file with changes, give different ID chain letters for water molecule and the metal ions otherwise ADT will combine this molecules with bonds to residues in the enzyme.
- Then turn to the ADT interface, open the ligand and save as PDBQT.
- Open the macromolecule and ligand.
- Grid→Macromolecule→Choose→Select Molecule
- Grid→Set map types→Choose Ligand

- Grid→Grid Box→Coordinates→x: 32.00
  y: 72.00
  z: 31.00
- Choose this coordinate for our enzyme (it can be changed for any other molecule).
- Grid Box dimensions: 80x80x80 (Again this can be changeable for any other process).
- File→Close saving current session
- Grid→Output→Save GPF
- Grid→Edit→GPF

- Running the autogrid4:

- autogrid4 –p *.gpf –l *.glg

**B.2 For Docking**

- Docking→Macromolecule→Set rigid→choose the PDBQT file as you prepared
- Docking→Ligand→Choose→Your ligand→Select Ligand
- Docking→Search→Genetic A
- Docking→Output→Lamarce A→*.DPF

- Running AutoDock4:

- Autodock4 –p *.dpf –l *.dlg

**B.3. Extracting RMSD values from a dlg file of AutoDock4**

- grep -A 1 RANKING rmsd.dat | cut -f 2,4,6 -d "_" | grep -v "\-\-" | grep -v "\-_">
- tmp.txt

- This command will create a temporary file called as tmp.txt.

- Open this file with "vi tmp.txt" command and write:
  :1,1008s/_merge.dlg-/ /g
  :1,1008s/RANKING//g

- Save the file. (:wq!)

- Then again give these commands:
  grep " " tmp.txt > tmp1.txt
  cut -f 2 -d "_" tmp1.txt > tmp2.txt

- There will be 7 columns in the tmp2.txt file:

  1.column: ID number of the ligand
  2. column: Rank
  3. column: SubRank
  4. column: Run
  5. column: Binding Energy
  6. column: Cluster RMSD
  7. column: Reference RMSD

- Then to extract the information from 1st, 4th and 7th columns we used a C program
- (rmsd_min.c). This program will read 1st, 4th and 7th columns from the tmp2.txt file,
- for each ligand it extracts the run which has the lowest rmsd values and write the
- results in rmsd_min.dat file in 3 columns:
  1.column: ligand id
  2.column: run number
  3.column: rmsd value

- Program is suitable for rmsd < 1.0 if you want to change it, you should change the
- value 1.0 to any number which you want in the line 44.
- if (n_r[i]<1.0){

- To compile the program write these commands:
- gcc rmsd_min.c
  ./a.out

**B.4. C program: rmsd_min.c**

(To extract the information from 1st,4th, and 7th columns, to obtain rmsd values from *.dlg files)

```
#include <stdio.h>
#include <stdlib.h>
#include <math.h>

int main(int argn, char *arg[]) {
  FILE *fd, *fp;
  char line[1024];
  double x, y, z, k;
  double l, m, n;
  double nsmall, n_r[2000];
  double run, id, run_r[2000], id_r[2000];
  int i, j;

  fd = fopen("tmp2.txt","r");

  fp = fopen("rmsd_min.dat","w");

  i = j = 0;
  nsmall=10000;

  while (fgets(line, 1024, fd)) {
    if (sscanf(line, "%lf %lf %lf %lf %lf %lf %lf", &x, &y, &z, &k, &l, &m, &n)==7) {
       //printf("%lf %lf %lf %lf %lf %lf %lf\n", &x, &y, &z, &k, &l, &m, &n);
       if (n<=nsmall) {
         nsmall = n;
```

```
        run = k;
        id = x;
        //printf("%lf %lf %lf\n",nsmall,run,id);
       }
       ++i;
       if (i==10) {
        run_r[j]=run;
        id_r[j]=id;
        n_r[j]=nsmall;
        ++j;
        i=0;
        nsmall=10000;
       }
    }
  }

  i=0;
  for (i=0;i<100;i++) {
    if (n_r[i]<1.0) {
      fprintf(fp,"%10.3lf %10.3lf %10.3lf\n", id_r[i],run_r[i],n_r[i]);
    }
  }

  return 0;
}
```

### B.5. Extracting $K_i$ (dissociation constant) values from dlg File

- There will be another C program which is called rmsd_$K_i$_min.c

Run the program with tmp2.txt file. You can obtain 5 output file:

i. rmsd_min_all.dat,

ii. rmsd_min.dat,

iii. $K_i$_min_all.dat,
iv. $K_i$_min.dat,
v. $K_i$_rmsd_all.dat.

- rmsd_min_all.dat and rmsd_min.dat files take the run which have the lowest rmsd value among the 10 run.

- $K_i$_min_all.dat and $K_i$_min.dat files take the lowest energy values (so lowest $K_i$ values) among the 10 run.

- In the rmsd_min.dat file, there are molecules that have the rmsd values only lower than 1.0.

- In $K_i$_min.dat file, there are molecules that have energy values only lower than 10.0 kcal/mol.

- But the files with "all" extension contain all molecules.

- In all of these 4 files, you can see a table of sample id, run id, RMSD, energy and $K_i$ values.

- In 5$^{th}$ file, $K_i$_rmsd_all.dat, there are 6 column. These are:
  1. column: RMSD (min RMSD)
  2. column: $K_i$ (belongs to min RMSD)
  3. column: energy (belongs to min RMSD)
  4. column: RMSD (min $K_i$)
  5. column: $K_i$ (belongs to min $K_i$)
  6. column: energy (belongs to min $K_i$)

**B.6. C program: rmsd_Ki_min.c**

(To extract Ki values from *.dlg files)

```
#include <stdio.h>
#include <stdlib.h>
#include <math.h>

int main(int argn, char *arg[]) {
  FILE *fd, *fp, *fp1, *fp2, *fp3, *fp4;
  char line[1024];
  double x, y, z, k;
  double l, m, n;
  double nsmall, n_r1[2000], n_r2[2000], eg, eg_r1[2000], Ki1[2000], eg_r2[2000],
Ki2[2000], Ki1all[2000], Ki2all[2000];
  double run, id, run_r[2000], id_r[2000];
  int i, j;

  fd = fopen("tmp2.txt","r");

  fp = fopen("rmsd_min.dat","w");
  fp1 = fopen("rmsd_min_all.dat","w");

  i = j = 0;
  nsmall=10000;

  // gets the smallest rmsd result in the cluster and its corresponding information

  while (fgets(line, 1024, fd)) {
    if (sscanf(line, "%lf %lf %lf %lf %lf %lf %lf", &x, &y, &z, &k, &l, &m, &n)==7) {
        if (n<=nsmall) {
          nsmall = n;
          run = k;
          id = x;
```

```
    eg = l;
       }
       ++i;
       if (i==10) {
         run_r[j]=run;
         id_r[j]=id;
         n_r1[j]=nsmall;
    eg_r1[j]=eg;
         ++j;
         i=0;
    nsmall=10000;
      }
    }
  }

  fprintf(fp, "sample_id   run_id     RMSD     energy        Ki\n");
  fprintf(fp, "                              kcal/mol    microMolar\n");
  fprintf(fp1, "sample_id   run_id     RMSD     energy        Ki\n");
  fprintf(fp1, "                              kcal/mol    microMolar\n");
  i=0;
  for (i=0;i<100;i++) {
    // print out the rmsd values smaller than 1.0 Angstrom.
    if (n_r1[i]<1.0) {
      Ki1[i] = exp(eg_r1[i]*1000/298/1.987)*1000000.0; // convert to microMolar units
      fprintf(fp,"%8.1lf %8.2lf %10.3lf %10.3lf %10.3lf\n",
id_r[i],run_r[i],n_r1[i],eg_r1[i],Ki1[i]);
    }
    // print out all the results
    Ki1all[i] = exp(eg_r1[i]*1000/298/1.987)*1000000.0; // convert to microMolar units
    fprintf(fp1,"%8.1lf %8.2lf %10.3lf %10.3lf %10.3lf\n",
id_r[i],run_r[i],n_r1[i],eg_r1[i],Ki1all[i]);
  }
```

```
//////////////

fclose(fd);
fd = fopen("tmp2.txt","r");
fp2 = fopen("Ki_min.dat","w");
fp3 = fopen("Ki_min_all.dat","w");

i = j = 0;

// gets the smallest energy(Ki) result in the cluster and its corresponding information

while (fgets(line, 1024, fd)) {
  if (sscanf(line, "%lf %lf %lf %lf %lf %lf %lf", &x, &y, &z, &k, &l, &m, &n)==7) {
    if (i==0) {
      n_r2[j] = n;
      run_r[j] = k;
      id_r[j] = x;
      eg_r2[j] = l;
      ++j;
    }
    ++i;
    if (i==10) i=0;
  }
}

// print out the energy values smaller than -10. kcal/mol.
fprintf(fp2, "sample_id   run_id    RMSD    energy       Ki\n");
fprintf(fp2, "                          kcal/mol    microMolar\n");
fprintf(fp3, "sample_id   run_id    RMSD    energy       Ki\n");
fprintf(fp3, "                          kcal/mol    microMolar\n");
i=0;
for (i=0;i<100;i++) {
  if (eg_r2[i]<-10.0) {
```

```
   Ki2[i] = exp(eg_r2[i]*1000/298/1.987)*1000000.0; // convert to microMolar units
   fprintf(fp2,"%8.1lf %8.2lf %10.3lf %10.3lf %10.3lf\n",
id_r[i],run_r[i],n_r2[i],eg_r2[i],Ki2[i]);
    }
   Ki2all[i] = exp(eg_r2[i]*1000/298/1.987)*1000000.0; // convert to microMolar units
   fprintf(fp3,"%8.1lf %8.2lf %10.3lf %10.3lf %10.3lf\n",
id_r[i],run_r[i],n_r2[i],eg_r2[i],Ki2all[i]);
  }

  fp4 = fopen("Ki_rmsd_all.dat","w");
  for (i=0;i<100;i++) {
   fprintf(fp4,"%10.3lf %10.3lf %10.3lf %10.3lf %10.3lf %10.3lf\n",
n_r1[i],Ki1all[i],eg_r1[i], n_r2[i],Ki2all[i],eg_r2[i]);
  }

  return 0;
}
```

### B.7. Tutorial for High-Throughput Virtual Screening with AutoDock4

**Step 1**. First, make sure that *python2.5* is already installed in your computer. If you can run AutoDock Tools, then you have already installed it.

**Step 2**. Create a directory (e.g., *myfirst_VS/*) and copy the following nine files into that directory:

1. vs1.sh
2. vs2.sh
3. vs3.sh
4. vs4.sh
5. examine_ligand_dict.py
6. prepare_dpf4.py
7. prepare_ligand4.py

8. prepare_ligand_dict.py
9. split_multi_mol2_file.py

**Step 3.** Assign the correct permissions to your files listed above, by giving the following command while located in *myfirst_VS/*.

chmod 755 *

**Step 4.** Run the first script file:

./vs1.sh

This will create a subdirectory called *VirtualScreening/* under your *myfirst_VS/* and three more subdirectories called, *Receptor/*, *etc/* and *Ligands/* under *VirtualScreening/.* Check if they really exist.

**Step 5.** Copy all your ligand files in .pdb format to *VirtualScreening/Ligands/*

**Step 6.** Run the second script file:

./vs2.sh

This will create new ligand files in .pdbqt format in *VirtualScreening/Ligands/.* Edit one of the .pdbqt file, just to check its content.

**Step 7.** Edit the file "*summary.txt*" under *VirtualScreening/etc/* that was created in Step 5 and get the information about all the different atom types present in your set of ligands by reading the first lines of *summar.txt* given as follows:
VirtualScreening ZINC subset summary as of Wed Apr 29 14:02:33 2009
There are 9 atom_types: ['A', 'C', 'F', 'NA', 'Cl', 'OA', 'N', 'Br', 'HD']
Here are some categories:
…
…

…

**Step 8.** Using AutoDock tools, prepare your grid parameter file for one of the ligands. Then edit your parameter file and on the line, which starts as *ligand types*, insert any additional atom types that you got from "summary.txt" in Step 6. Also, define *atom-specific affinity map* for each new atom type. To demonstrate;

npts 74 50 60 # num.grid points in xyz
gridfld conf_high_6b.maps.fld # grid_data_file
spacing 0.375 # spacing(A)
receptor_types A C H HD N OA SA # receptor atom types
ligand_types C HD N NA OA # ligand atom types
receptor conf_high_6b.pdbqt # macromolecule
gridcenter 3.6 36.9 17.42 # xyz-coordinates or auto
smooth 0.5 # store minimum energy w/in rad(A)
map conf_high_6b.C.map # atom-specific affinity map
map conf_high_6b.HD.map # atom-specific affinity map
map conf_high_6b.N.map # atom-specific affinity map
map conf_high_6b.NA.map # atom-specific affinity map
map conf_high_6b.OA.map # atom-specific affinity map
elecmap conf_high_6b.e.map # electrostatic potential map
dsolvmap conf_high_6b.d.map # desolvation potential map

To add the atom "F" found in *summary.txt* file, simply make the changes highlighted below:

npts 74 50 60 # num.grid points in xyz
gridfld conf_high_6b.maps.fld # grid_data_file
spacing 0.375 # spacing(A)
receptor_types A C H HD N OA SA # receptor atom types
ligand_types C HD N NA OA **F** # ligand atom types
receptor conf_high_6b.pdbqt # macromolecule
gridcenter 3.6 36.9 17.42 # xyz-coordinates or auto
smooth 0.5 # store minimum energy w/in rad(A)
map conf_high_6b.C.map # atom-specific affinity map
map conf_high_6b.HD.map # atom-specific affinity map
map conf_high_6b.N.map # atom-specific affinity map

map conf_high_6b.NA.map # atom-specific affinity map
map conf_high_6b.OA.map # atom-specific affinity map
**map conf_high_6b.F.map # atom-specific affinity map**
elecmap conf_high_6b.e.map # electrostatic potential map
dsolvmap conf_high_6b.d.map # desolvation potential map

**Step 9.** Run your *autogrid* to create your map files.

**Step 10.** Copy your receptor's pdbqt file and all your map files you just created in Step 8, into *VirtualScreening/Receptor/*

**Step 11.** Make sure that your receptor file's base name matches your map files' base names. For example, if your receptor file is called as ***lsd1***.*pdbqt*, then your map files' names should start with ***lsd1***.*A.map*, ***lsd1***.*C.map*, etc..

**Step 12.** Edit the script file *vs3.sh*, and make the necessary modifications as highlighted below:

```
for f in `ls ../Ligands/*.pdbqt`; do
name=`basename $f .pdbqt`
echo $name
mkdir "$name"_1RO6
cd "$name"_1RO6
cp ../"$f" .
ln -s ../../Receptor/1RO6.pdbqt .
ln -s ../../Receptor/1RO6*map* .
$VSTROOT/prepare_dpf4.py -l `basename $f` -r 1RO6.pdbqt \
-p ga_num_evals=5000000 \
-p ga_pop_size=200 \
-p ga_run=10 \
-p rmstol=2.0
cd ..
done
```

**Step 13.** Run the script file:

./vs3.sh

This will create a directory for each ligand, which will contain all the necessary files for docking calculations; map files for each atom type, receptor's pdbqt file and the docking parameter file. *Note: map files are not really located in that directory, but in VirtualScreening/Receptor/. They are simply linked to that location.*

**Step 14.** Run the script file:

./vs4.sh

This will start the docking calculations one at a time.
*Note: If you want to parallelize your job, then you have to create another directory like myfirst_VS/ and start over the steps 1-12.*

*Extracting Information from *.dlg File*

# REFERENCES


1. Butcher, R.W. and E.W. Sutherland, "Adenosine 3', 5'-Phosphate in Biological Materials", J. *Biol. Chem.,* Vol. 237, pp. 1244-1250, 1962.

2. Torphy, T.J., "Phosphodiesterase isozymes: molecular targets for novel antiasthma agents", *Am. J. Respir. Crit. Care Med*., Vol. *157*, pp. 351–370, 1998.

3. Conti, M., and S.L. Jin, "The molecular biology of cyclic nucleotide phosphodiesterases", *Prog. Nucleic Acid Res. Mol. Biol*., Vol. *63*, pp. 1-38, 1999.

4. Soderling, S.H., and J.A. Beavo, "Regulation of cAMP and cGMP signaling: new phosphodiesterases and new functions", *Curr.Opin. Cell Biol.*, Vol. 12, pp. 174–179, 2000.

5. Houslay, M.D., and G. Milligan, "Tailoring cAMP-signalling responses through isoform multiplicity", *Trends Biochem. Sci.,* Vol. 22, pp. 217–224, 1997.

6. Houslay, M.D., M. Sullivan, and G.B. Bolger, "The multienzyme PDE4 cyclic adenosine monophosphate-specific phosphodiesterase family: intracellular targeting, regulation, and selective inhibition by compounds exerting anti-inflammatory and antidepressant actions", *Adv. Pharmocol.,* Vol. 44, pp. 225–343, 1998.

7. Antoni, F., "Molecular diversity of cyclic AMP signaling", *Front.Neuroendocrinol.* Vol. 21, pp. 103–132, 2000.

8. Three-Dimensional Structures of PDE4D in Complex with Roliprams and Implication on Inhibitor Selectivity, *Structure.* 2003 July;11:865-73.

9. Corbin, J.D., and S.H. Francis, "Cyclic GMP phosphodiesterase-5: target of sildenafil", *J. Biol. Chem.,* Vol. 274, pp. 13729–13732, 1999.

10. Manganiello, V.C., M. Taira, F. Degerman, and P. Belfrage, “Type III cGMP-inhibited cyclic nucleotide phosphodiesterase (PDE3 gene family)”, *Cell. Signal.*, Vol 7, pp. 445–455, 1995.

11. Mehats, C.M., C.B. Anderson, M. Filopanti, S.L.C. Jin, and M. Conti, “Cyclic nucleotide phosphodiesterases and their role in endocrine cell signaling”, *Trends Endocrinol. Metab.*, Vol. 13, pp. 29–35, 2002.

12. Müller, T., P. Engels, and J.R. Fozard, “Subtypes of type 4 cAMP phosphodiesterase: structure, regulation and selective inhibition”, *Trends Pharmacol. Sci.*, Vol. 17, pp. 294–298, 1996.

13. Thompson, W.J., “Cyclic nucleotide phosphodiesterases: pharmacology, biochemistry and function”, *Pharmacol. Ther.*, Vol. 51, pp. 13–33, 199.

14. Manallack D.T., R.A. Hughes, P.E. Thompson, “The next generation of phosphodiesterase inhibitors: structural clues to ligand and substrate selectivity of phosphodiesterases”, *Journal of Medicinal Chemistry,* Vol. 48,No. 1, pp. 3449-3462, 2005.

15. Reilly, M.P., and E.R. Mohler, “III. Cilostazol: treatment of intermittent claudication”, *Ann. Pharmacother.*, Vol. *35*, pp. 48–56, 2001.

16. Rotella, D.P., “Phosphodiesterase 5 inhibitors: current status and potential applications”, *Nat. Rev. Drug Discov.*, Vol. 1, pp. 674–682, 2002.

17. Giembycz, M.A., “Phosphodiesterase 4 inhibitors and the treatment of asthma”, *Drugs,* Vol. 59, pp. 193–212, 2000.

18. Souness, J.E., D. Aldous, and C. Sargent, “Immunosuppressiveand anti-inflammatory effects of cyclic AMP phophodiesterase (PDE) type 4 inhibitors”, *Immunopharmacology,* Vol. 47, pp. 127–162, 2000.

19. Huang, Z., Y. Ducharme, D. Macdonald, and A. Robichaud, " The next generation of PDE4 inhibitors", *Curr. Opin. Chem. Biol.,* Vol. 5, pp. 432-438, 2001.

20. Giembycz, M.A., "Development status of second generation PDE 4 inhibitors for asthma and COPD: the story so far", *Monaldi Arch. Chest Dis.,*Vol. 57, pp. 48–64, 2002.

21. Piaz, V.D., "Phosphodiesterase 4 inhibitors, structurally unrelated to rolipram, as promising agents for the treatment of asthma and other pathologies", *Eur. J. Med. Chem.*, Vol. 35, pp. 463–480, 2000.

22. Barnette, M.S., and D.C. Underwood, "New phosphodiesterase inhibitors as therapeutics for the treatment of chronic lung disease", *Curr. Opin. Pulm. Med,* Vol. 6, pp. 164–169, 2000.

23. Sturton, G., and M. Fitzgerald, "Phosphodiesterase 4 inhibitors for the treatment of COPD", *Chest,* Vol. 121, pp. 192–196, 2002.

24. Bobon, D., "Is phosphodiesterase inhibition a new mechanism of antidepressant action? A double-dummy study between rolipram and desipramine in hospitallized major and/or endogenous depressives", *Eur. Arch. Psychiatry Neurol. Sci.,* Vol. 238, pp. 2–6, 1988.

25. Scott, A.I., A.F. Perini, P.A. Shering, and I.L. Whalley, "Inpatient major depression: is rolipram as effective as amitriptyline?", *Eur. J. Clin. Pharmacol.,* Vol. 40, pp. 127–129, 1991.

26. Castro, A., "Cyclic nucleotide phosphodiesterases and their role in immunomodulatory responses: advances in the development of specific phosphodiesterase inhibitors", *Med. Res. Rev.*, Vol. 25, pp. 229–244, 2005.

27. Ariga, M., "Nonredundant function of phosphodiesterases 4D and 4B in neutrophil recruitment to the site of inflammation", *J. Immunol.*, Vol. 173, pp. 7531–7538, 2004.

28. Jin, S.L. and M. Conti, "Induction of the cyclic nucleotide phosphodiesterase

PDE4B is essential for LPS-activated TNF-alpha responses" , *Proc. Natl. Acad. Sci. U. S. A.,* Vol. 99, pp. 7628–7633, 2002.

29. Jin, S.L., "Impaired growth and fertility of cAMP-specific phosphodiesterase PDE4D deficient mice", *Proc. Natl. Acad. Sci. U. S. A.,* Vol. 96, pp. 11998–12003, 1999.

30. Mehats, C., "PDE4D plays a critical role in the control of airway smooth muscle contraction", *FASEB J.,* Vol. 17, pp. 1831–1841, 2003.

31. Zhang, H.T., Y. Huang, S.L. Jin, S.A. Frith, N. Suvarna, M. Conti, J.M. O'Donnell, "Antidepressant-like profile and reduced sensitivity to rolipram in mice deficient in the PDE4D phosphodiesterase", *Neuropsychopharmacology.*, Vol 27, No. 4, pp. 587- 595, 2002.

32. Lynch, M.J., "RNA silencing identifies PDE4D5 as the functionally relevant cAMP phosphodiesterases interacting with β- arrestin to control switching of the β2-adrenergic receptor to activation of ERK in HEK293 cells", *J. Biol. Chem.,*Vol. 280, pp. 33178-33189, 2005.

33. McCahill, A., "In resting COS1 cells a dominant negative approach shows that specific, anchored PDE4 cAMP phosphodiesterase isoforms gate the activation, by basal cyclic AMP production, of AKAP-tethered protein kinase A type II located in the centrosomal region", *Cell. Signal.,* Vol. 17, pp. 1158–1173, 2005.

34. Banner, K.H. and M.A. Trevethick, "PDE4 inhibition: a novel approach for the treatment of inflammatory bowel disease", *Trends Pharmacol. Sci.,* Vol. 25, pp. 430–436, 2004.

35. Draheim, R., "Anti-inflammatory potential of the selective phosphodiesterase 4 inhibitor N-(3,5-dichloro-pyrid-4-yl)-[1-(4- fluorobenzyl)-5-hydroxy-indole-3-yl]-

gly oxylic acid amide (AWD 12-281), in human cell preparations", *J. Pharmacol. Exp. Ther.,* Vol. 308, pp. 555–563, 2004.

36. Jeffery, P., "Phosphodiesterase 4-selective inhibition: novel therapy for the inflammation of COPD", *Pulm. Pharmacol. Ther.,* Vol. 18, pp. 9-17, 2005.

37. O'Donnell, J.M. and H.T. Zhang, "Antidepressant effects of inhibitors of cAMP phosphodiesterase (PDE4)", *Trends Pharmacol. Sci.,* Vol. 25, 158–163, 2004.

38. Spina, D., "The potential of PDE4 inhibitors in respiratory disease", *Curr. Drug Targets Inflamm. Allergy,* Vol. 3, pp. 231–236, 2004.

39. Scotland, G., M. Beard, S. Erdogan, E. Huston, F. McCallum, S. J. MacKenzie; A. H. Peden, L. Pooley, N. G. Rena, A. H. Ross, S. J. Yarwood, M. D. Houslay, "Differential regulation of mesangial cell mitogenesis by cAMP phosphodiesterase isozymes 3 and 4", *Methods,* Vol. 14, pp. 65-79, 1998.

40. Verghese, M. W., R. T. McConnell, J. M. Lenhard, L. Hamacher, S. L. Jin, *Mol. Pharmacol.,* Vol. 47, pp. 1164-1171, 1995.

41. Phosphodiesterase 4 Inhibitors for the Treatment of Asthma and COPD.

42. Houslay, M.D. and D.R. Adams, "PDE4 cAMP phosphodiesterases: modular enzymes that orchestrate signalling cross-talk, desensitization and compartmentalization", *Biochem. J.,* Vol. 370, pp. 1–18, 2003.

43. Conti, M., "Cyclic AMP-specific PDE4 phosphodiesterases as critical components of cyclic AMP signaling", *J. Biol. Chem.,* Vol. 278, pp. 5493–5496, 2003.

44. MacKenzie, S.J., "Long PDE4 cAMP specific phosphodiesterases are activated by protein kinase A-mediated phosphorylation of a single serine residue in Upstream Conserved Region 1 (UCR1)", *Br. J. Pharmacol.,* Vol. 136, pp. 421–433, 2002.

45. Sette, C. and M. Conti, "Phosphorylation and activation of a cAMP-specific phosphodiesterase by the cAMP-dependent protein kinase. Involvement of serine 54 in the enzyme activation", *J. Biol. Chem.,* Vol. 271, pp. 16526–16534, 1996.

46. Oki, N., "Short term feedback regulation of cAMP in FRTL-5 thyroid cells. Role of PDE4D3 phosphodiesterase activation", *J. Biol. Chem.,* Vol. 275, pp. 10831–10837, 2000.

47. Baillie, G.S., "Sub-family selective actions in the ability of Erk2 MAP kinase to phosphorylate and regulate the activity of PDE4 cyclic AMP-specific phosphodiesterases", *Br. J. Pharmacol.,* Vol. 131, pp. 811–819, 2000.

48. Hoffmann, R., "The MAP kinase ERK2 inhibits the cyclic AMP-specific phosphodiesterase HSPDE4D3 by phosphorylating it at Ser579.", *EMBO J.,* Vol. 18, pp. 893–903, 1999.

49. MacKenzie, S.J., "ERK2 mitogenactivated protein kinase binding, phosphorylation, and regulation of the PDE4D cAMP-specific phosphodiesterases. The involvement of COOH-terminal docking sites and NH2-terminal UCR regions", *J. Biol. Chem.,* Vol. 275, pp. 16609–16617, 2000.

50. Houslay M.D., P. Schafer and K.Y.J.Zhang, "Keynote review: Phosphodiesterase-4 as a therapeutic target", *DDT* , Vol. 10, No. 22 , 2005.

51. Zhang, K.Y.J., "A glutamine switchmechanism for nucleotide selectivity by phosphodiesterases", *Mol. Cell,* Vol. 15, pp. 279–286, 2004.

52. Card, G.L., "Structural Basis for the Activity of Drugs that Inhibit Phosphodiesterases", *Structure,* Vol. 12, pp. 2233–2247, 2004.

53. Schwabe, U., "4-(3-Cyclopentyloxy-4-methoxyphenyl)-2-pyrrolidone (ZK 62711): a potent inhibitor of adenosine cyclic 3$,5$-monophosphate phosphodiesterases

inhomogenates and tissue slices from rat brain" , *Mol. Pharmacol.,* Vol. 12, pp. 900–910, 1976.

54. Lipworth, B.J., "Phosphodiesterase-4 inhibitors for asthma and chronic obstructive pulmonary disease", *Lancet,* Vol. 365, pp. 167–175, 2005.

55. Lee, M.E., "Crystal structure of phosphodiesterase 4D and inhibitor complex", *FEBS Lett.,* Vol. 530, pp. 53–58, 2002.

56. Xu, R.X., "Crystal structures of the catalytic domain of phosphodiesterase 4B complexed with amp 8-br-AMP, and rolipram", *J. Mol. Biol.,* Vol. 337, pp. 355–365, 2004.

57. Huai, Q. *,* "Three-dimensional structures of PDE4D in complex with roliprams and implication on inhibitor selectivity", *Structure (Camb),* Vol. 11, pp. 865–873, 2003.

58. Huai, Q., "Crystal structures of phosphodiesterases 4 and 5 in complex with inhibitor 3-isobutyl-1-methylxanthine suggest a conformation determinant of inhibitor selectivity", *J. Biol. Chem.,* Vol. 279, pp. 13095–13101, 2004.

59. Rocque, W.J., "Human recombinant phosphodiesterase 4B2B binds (R)-rolipram at a single site with two affinities", *Biochemistry,* Vol. 36, pp. 14250–14261, 1997.

60. Leach, A.R., V.J. Gillet, "An Introduction to Chemoinformatics", *Springer,* 2007.

61. Charifson, P.S. and W.P. Walters, "Filtering Databases and Chemical Libraries", *Molecular Diversity,* Vol. 5, pp. 185–197, 2000.

62. Wilton, D., P. Willett, K. Lawson and G. Mullier, "Comparison of Ranking Methods for Virtual Screening in Lead-Discovery Programmes", *Journal of Chemical Information and Computer Sciences,* Vol. 43, pp. 469–474, 2003.

63. Thornber, C.W. "Isosterism and MolecularModification in Drug Design", *Chemical Society Reviews*, Vol. 8, pp. 563–580, 1979.

64. Langer, T., and R.D. Hofmann, "Pharmacophores and Pharmacophore Searches", *Wiley-Vch*., Vol. 32, 2006.

65. Wermuth, C. G., C. R. Ganellin, P. Lindberg, and L. A. Mitscher, "Glossary of terms used in medicinal chemistry (IUPAC Recommendations 1997). *Annu. Rep. Med. Chem.*, Vol. *33*, pp. 385–395, 1998.

66. Wermuth, C. G., and T. Langer, "Pharmacophore identification in *3D QSAR in Drug Design. Theory Methods and Applications*", Kubinyi, H. (ed.). ESCOM, Leiden, pp. 117–136, 1993.

67. Schneider, G., T. Giller, W. Neidhart, G. Schmid, "Scaffold-hopping by topological pharmacophore search: a contribution to virtual screening." *Angew. Chem. Int. Ed.*, Vol. *38*, pp. 2894–2896, 1999.

68. Rognan, D., T. Boulanger, R. Hofmann, D.P. Vercauteren, J. M. Andre, F. Durant, C. G. Wermuth, "Structure and molecular modeling of GABAA antagonists", *J. Med. Chem.*, Vol. *35*, pp. 1969–1977, 1992.

69. Ariëns, E. J., J.F. Rodrigues de Miranda, A.M. Simonis, " The pharmacon-receptor–effector concept: a basis for understanding the transmission of information in biological systems", *In The Receptors*, pp. 33–91, 1979.

70. Wermuth, C. G., "Aminopyridazines–an alternative route to potent muscarinic agonists with no cholinergic syndrome", *Farmaco*, Vol. 48, pp. 253–274, 1993.

71. Rognan, D., P. Sokoloff, A. Mann, M.P. Martres, J.C. Schwartz, J.Costentin, C.G. Wermuth, "Optically active benzamides as predictive tools for mapping the dopamine D2 receptor", *Eur. J. Pharmacol. Mol. Pharmacol. Sect.*, Vol. 3, pp. 59–70, 1990.

72. Roche, O., P. Schneider, J. Zuegge, W. Guba, M. Kansy, A. Alanine, K. Bleicher, F. Danel, E-M. Gutknecht, M. Rogers-Evans, W. Neidhart, H. Stalder, M. Dillon, E. Sjögren, N. Fotouhi, P. Gillespie, R. Goodnow, W. Harris, P. Jones, M. Taniguchi, S. Tsujii, W. von der Saal, G. Zimmermann and G. Schneider, "Development of a Virtual Screening Method for Identification of "Frequent Hitters" in Compound Libraries", *Journal of Medicinal Chemistry,* Vol. 45, pp. 137–142, 2002.

73. Lipinski, C.A., F. Lombardo, B.W. Dominy and P.J. Feeney, "Experimental and Computational Approaches to Estimate Solubility and Permeability in Drug Discovery and Development Settings", *Advanced Drug Delivery Reviews*, Vol. 23, pp. 3–25, 1997.

74. Oprea, T.I., "Property Distributions of Drug-Related Chemical Databases", *Journal of Computer-Aided Molecular Design,* Vol.14, pp. 251–264, 2000.

75. Tice, C. M., "Selecting the Right Compounds for Screening: Does Lipinsk's Rule of 5 for Pharmaceuticals Apply to Agrochemicals?", *Pest Management Science,* Vol. 57, pp. 3–16, 2001.

76. Young, D.C., "Computational Drug Design: A Guide for Computational and Medicinal Chemists" , 2009.

77. Böhm, H-J. and G. Klebe, "What can We Learn from Molecular Recognition in Protein–Ligand Complexes for the Design of New Drugs?", *Angewandte Chemie* (*International ed. İn English*), Vol. 35, pp. 2588–2614, 1996.

78. Ajay, A. and M.A. Murcko, "Computational Methods to Predict Binding Free Energy in Ligand–Receptor Complexes", *Journal of Medicinal Chemistry,* Vol. 38, pp. 4951–4967, 1995.

79. Boström, J., P-O. Norrby, and T. Liljefors, “Conformational Energy Penalties of Protein-Bound Ligands”, *Journal of Computer-Aided Molecular Design,* Vol. 12, pp. 383–396, 1998.

80. Wolber, G., and T. Langer, “LigandScout: 3-D Pharmacophores Derived from Protein-Bound Ligands and Their Use as Virtual Screening Filters”, *J. Chem. Inf. Model.*, Vol. 45, No. 1, pp. 160-169, 2005.

81. Morris, G.M., D.S. Goodsell, R.S. Halliday, R. Huey, W.E. Hart, R.K. Belew, and A.J. Olson, “Automated Docking Using a Lamarckian Genetic Algorithm and and Empirical Binding Free Energy Function.”, *J Comp Chem*, Vol. 19, pp. 1639-1662, 1998.